Can We Work More Safely and Healthily with Robot Partners? A Human-Friendly Robot-Human Coordinated Order Fulfillment Scheme[1]

*Jiuh-Biing Sheu[2], Tsan-Ming Choi[3]**

Abstract: This work addresses the issue of intelligent robot-human coordinated parts-to-picker order fulfillment carried out in a human-friendly manner. One unique feature of the proposed approach involves integrating a real-time data-driven stochastic-dynamic model with a fatigue accumulation function. The optimal solutions help achieve coordination between human pickers and robots such that robots agilely adapt to the coordinated pickers' efficiency and fatigue conditions. Specifically, the proposed method estimates human pickers' instantaneous performance and robot queue lengths, which are then fed back in real time as indexes to adjust robots' speeds of handling racks and moving them to human pickers. Using data that are provided by a giant electronic-commerce company, our analyses demonstrate that the proposed robot-picker coordination system permits alleviating a picker's fatigue without much influence on picking efficiency. In particular, a picker's accumulated fatigue can be reduced by 53.74% at the expense of lowering picker efficiency by 14.79% if the proposed robot-picker coordination system is applied in the focal firm of the study case. Through our scenario design and sensitivity analysis, additional findings and insights, including the rules of human-friendly robot behaviors for coordination with human pickers in different operational scenarios are provided. They facilitate the development of "human-friendly" intelligent robot-human coordinated order-fulfillment systems for intelligent logistics operations.

***Keywords**:* Intelligent logistics; Automated warehousing system; Mobile rack; Robot-human coordination; Data-driven stochastic optimal control.

History: Received: February 2022; Accepted: October 2022 by Panos Kouvelis, after two revisions.

1. INTRODUCTION

Business operations have entered the Industry 4.0 era in which robotics are widely applied in the production, logistics, and e-commerce companies (Olsen and Tomlin 2020; Rai *et al.* 2021; Loffler *et al*., 2021; Choi *et al*. 2022). This is evidenced by the claims made by Amazon.com:

"*It's better for everybody…Workers no longer would have to walk massive warehouse floors to find the right power drill – instead, robots would bring the drill directly to them… The hour or more it took to process a package had been shaved down to as little as 15 minutes…Robots, Amazon insists, are good for workers… "They make the job safer,"…*" (Evans, 2020).

"*But picking three times faster also implies more wear and tear due to repetitive motion and working faster at*

[1] Acknowledgement: This study is partially supported by MOST project (code: MOST 109-2410-H-002-076-MY3).

[2] Department of Business Administration, National Taiwan University, Taipei, Taiwan (Email: jbsheu@ntu.edu.tw).

[3] Centre for Supply Chain Research, University of Liverpool Management School, Chatham Building, Liverpool L69 7ZH, the United Kingdom. Emails: tmjchoi@gmail.com; t.m.choi@liverpool.ac.uk. (* Corresponding author)

lifting and handling products… So along with the drive to automate more warehouse tasks comes much higher expectations for workers…The robots have raised the average picker's productivity from around 100 items per hour to what Mr. Long and others have said is a target of around 300 or 400, though the numbers vary across teams and facilities…" (Del Rey, 2019).

Indeed, there is no doubt that advancements in such disruptive technologies as robotics and related applications (Azadeh *et al*., 2019; Perera 2020; Chung, 2021; Shi *et al*., 2021; Wang *et al*. 2022) have brought new benefits to electronic-commerce (e-commerce) companies (such as Amazon, Alibaba, and JingDong) by increasing the efficiency of order fulfillment. However, they are simultaneously creating new safety challenges.

Order picking is a critical step in customer order fulfillment (Frazelle, 2002; de Koster *et al*. 2007; de Vries *et al*., 2016; Batt and Gallino, 2019). In a typical warehouse, it is not only costly and time-consuming but also labor-intensive. In general, the cost of order picking is estimated to account for more than 50% of the total warehousing cost (Tompkins *et al*., 2010). Furthermore, order picking typically relies on manual labors to retrieve multiple items from storage, sort them, and then package them to fulfill customer orders (de Koster *et al*. 2007; Chen *et al*., 2010; de Vries *et al*., 2016). Owing to the large variety of customer orders and stock keeping units (SKUs) in most e-commerce operations, each order picking task for a customer order is difficult to replicate. The ordering picking's efficiency and accuracy depend mainly on the human pickers' experience (Batt and Gallino, 2019) and performance (de Vries *et al*., 2016). Moreover, in e-commerce, agile order picking can be more challenging when the ordered products are diverse, demand is fluctuating, customer returns are increasing and customers expect more flexible and expeditious logistics services (Frazelle, 2002). Briefly, order picking, which depends on intensive labor and pickers' performance, remains crucial to the success of fulfilling customer orders with high service quality, regardless of the methods/technologies that are deployed in a warehouse.

Despite a variety of innovative automation technologies, such as autonomous mobile robots, have been increasingly introduced to carry out order fulfillment jointly with human pickers in warehouses (Banker, 2016; Tobe, 2018; Wang *et al*., 2022), "parts-to-picker" order fulfillment systems raise several new issues on humanity and safety. This creates a challenge on robot-human coordination. A certain number of robots that carry racks automatically from the storage area to the order picking area may be deployed to facilitate the picking tasks of human pickers. Poor robot-human coordination typically increases the number of robots that carry, queue and await handling by pickers in the order picking area. Note that a human picker's efficiency is not as controllable as that of a robot, and may vary with time and her psychophysical condition. Thus, an unexpected delay in picking items may inevitably occur if robots just continue to carry racks to her and are unable to respond to her performance. More seriously, recent reports have revealed a substantial rising injury rates in automated warehouses (Al Elew and Oh, 2020; Doll, 2020; Evans, 2020). For example, Amazon's warehouse injury rates have increased every year since 2016 after they began using robots in parts-to-picker order fulfillment. The serious injury rate in 2019 was 7.7 injuries per 100 employees, which was 33% higher than in 2016 and nearly double the corresponding recent industry standard (Evans, 2020). Order picking often requires pickers to perform repetitive tasks in awkward postures for a whole day, easily causing musculoskeletal disorders

(Lavender *et al.*, 2012; Grosse *et al.*, 2015), which accounts for up to 33% of all injuries and illnesses in the US in 2013 (Bureau of Labor Statistics, 2014).

Motivated by the aforementioned robot-human coordination issues in parts-to-picker order fulfillment practices, this paper aims to answer the following questions.

(1) How should human pickers and coordinated robots react and adapt to each other to fulfill orders in a human-friendly manner considering robot-human collaboration?

(2) How does such a human-friendly robot-human coordination scheme affect the performance of an order fulfillment system in a parts-to-picker order fulfillment center? Specifically, what are the critical factors and how they influence the systems performance from humanity and safety perspectives?

To address the above research questions, we build a stochastic optimal control-based data-driven solution approach. We propose a robot-picker coordinated order fulfillment mechanism under which the robot and picker efficiencies have the following characteristics: (i) The robot and picker efficiencies can be effectively controlled and coordinated if real-time data concerning newly arriving racks are available and used. (ii) The robot efficiency heavily depends on real-time data concerning newly arriving racks whereas picker efficiency highly depends on the length of the queue of unprocessed racks. (iii) The picker-to-robot relative performance from the perspective of either efficiency or effectiveness during peak hours is less than that during either normal or off-peak hours. The picker-to-robot relative performance is best in the "off-peak" scenario. Moreover, we find that the robot efficiency is not the most important metric. Rather, human efficiency dominates the efficiency of a parts-to-picker order fulfillment system, particularly during peak hours. Accordingly, controlling the number of queued racks by slowing down their delivery by robots to the picking-packaging area is in fact a more efficient measure than slowing down the rack-processing of a picker (in order to alleviate that picker's fatigue); this is especially prominent during a peak-hour period. Last but not least, employing data that were provided by a well-established e-commerce company, our analyses demonstrate that a picker's accumulated fatigue can be reduced by over 50% at the expense of lowering picker efficiency by around 15% if the proposed robot-picker coordination system is applied.

The rest of this paper is organized as follows. Section 2 reviews the relevant literature to elucidate its contribution to the field of innovative logistics. Section 3 describes the problem and characterizes the proposed robot-picker coordinated order fulfillment system. Section 4 presents a proposed stochastic-dynamic optimal control model. Section 5 develops a real-time data-driven approach to estimating and controlling the state variables of the proposed robot-picker coordinated order fulfillment system. Section 6 presents the computational results of a practice-based real data analysis. Section 7 draws conclusions, provides managerial implications, and discusses future research. To enhance exposition, all technical proofs are put in an online appendix.

2. LITERATURE REVIEW

Recently, in the Industry 4.0 era, robotic technologies (such as Amazon robotics and Jingdong (JD) robots) that are used by e-commerce companies (Luo and Choi 2022) for parts-to-picker order fulfillment have emerged (Tam, 2014; Banker, 2016; Tobe, 2018; Shi *et al*., 2021). They have revolutionalized the way of order fulfillment operated in warehouses. Most of extant literature on parts-to-picker order fulfillment systems focuses mainly on increasing the warehousing efficiency utilizing diverse methodologies. For example, Enright and Wurman (2011) identified several parts-to-picker order fulfillment-related resource allocation problems, including order allocation and robot allocation problems. Recently, Boysen *et al*. (2017) proposed a mixed-integer programming model to minimize the number of rack visits to a stationary picking station in a mobile robot-based order-picking problem. The authors solved the optimization problem by first decomposing the problem into two sub-problems of rack sequencing (for a given order sequence) and order sequencing (for a given rack sequence). By contrast, Lamballais *et al*. (2017) proposed four queuing network models associated with various warehousing layouts and robot zoning strategies to analyze the performance of an automated storage and parts-to-picker system with the objectives of optimizing robot utilization, maximizing order throughput, and minimizing order cycle time. Differing from the above optimization-based analytical models, Bozer and Aldarondo (2018) utilized a simulation-based method to evaluate and compare the performances of two types of parts-to-picker picking systems (called "miniload" and "Kiva" systems) in the aspects of expected throughputs and expected container retrieval times in order processing. Some of the subsequent literature, including Weidinger *et al*. (2018) and Yuan *et al*. (2019), aimed at the problem of pod/rack storage which is the antecedent of parts-to-picker order fulfillment, where the inventory of items is stored and spread over multiple mobile pods that are carried by robots moving between storage and picking (stowing) zones. More recently, Wang *et al*. (2022) utilized an "approximate dynamic programming" (ADP) based branch-and-price approach to solving the optimal robot scheduling problem for parts-to-picker order fulfillment systems. Different from the above literature which solely focuses on efficiency, Wang *et al*. (2022) incorporated fluctuations of the working states of human pickers into the model, and hence, the human factor was explored. However, human safety was not yet examined by Wang *et al.* (2022). In addition, Boldrer *et al*. (2022) proposed a hierarchical framework to address the problem of multi-robot navigation in human-shared working environments. Even though the approach of Boldrer *et al*. does not aim at parts-to-picker order fulfillment systems, the authors' idea of conceptualizing a safe and socially-aware navigation in their proposed methodological framework is noteworthy, and consistent with our research goal.

Despite remarkable advances made to increase efficiency in parts-to-picker order fulfillment, issues such as safety and harmony in the human-robot interactions remain under-explored in relevant intralogistics operations and related areas (Enright and Wurman, 2011; Azadeh *et al*., 2019; Chen *et al*., 2022). As argued by Enright and Wurman (2011), systems optimization at the high level, considering dual objective functions for both workers and robots, remains challenging as these two objectives may not be compatible. Details of the operational features and challenges of parts-to-picker order fulfillment can also be found in Enright and Wurman (2011). Drawing from experimental results, Chen *et al*. (2022) further suggested the urgent necessity of developing novel robotic motion methods to ensure human safety for applications of human-robot coordination

in warehouses. Note that Azadeh *et al*. (2019) comprehensively reviewed the literature on robotized and automated warehouse systems. They pointed out that issues related to human-machine interaction in automated warehousing environments have not been fully addressed.

Another stream of relevant literature concerns the association of human factors with order picking performance (Grosse *at el*., 2015; de Vries *et al*., 2016; Grosse *et al*., 2017; Batt and Gallino, 2019; Loske, 2022). As argued by Grosse *et al*. (2017), human factors determine the performance of an order picking system, which is time-consuming and labor-intensive, but they are often ignored in management-oriented research. Incorporating human factors into order picking models for intralogistics operations and warehouse management is, thus, indispensable - particularly with respect to production, operations and logistics management (de Koster *et al*., 2007). Observe that the related literature can be divided into two categories: the first focuses on relevant aspects of human cognition (*e.g*., human learning) to improve productivity/efficiency, and the second cares about the welfare and health of workers. The corresponding literature reviews are detailed below.

Prior studies on cognition have investigated its impact on order picking performance. Some of them (Grosse and Glock, 2015) have integrated the concept of human learning (characterized by learning curves) with mathematical models to study how pickers' performance can be improved by learning from experience. de Vries *et al*. (2016) conducted a field experiment to examine three types of picker-to-parts order picking methods under two incentive schemes for pickers with different regulatory foci ("prevention-focus" vs. "promotion-focus"). The work of de Vries *et al*. (2016) is pioneering in "elaborately" aligning order picking methods, incentive mechanisms, and regulatory focus to bridge the gap between organizational behavior theories and warehousing practices. Batt and Gallino (2019) empirically estimated the effects of several factors, including a picker's learning from experience of walking and searching processes, on picking time for order fulfillment in online women's apparel retailing. One remarkable feature of their work is the empirical demonstration of the effects of pickers' heterogeneous learning capabilities, characterized by different learning curves, on order picking performance. Rather recently, Loske (2022) combined parametric and non-parametric approaches to analyze how the interactions between humans, machines, and intelligent software impact human learning and perception of work characteristics in the transition to an automated order picking system. The author's empirical findings verified that the real-time feedback provided by the order picking system can facilitate human learning by doing tasks in the perception–cognition–motor–action cycle, thus clarifying the need for human-centered work system design.

The literature on the welfare and health of order-picking workers aims to develop integrated models that consider both ergonomic (such as human energy expenditure and fatigue) and economic (such as picking time) performances in order picking (Grosse *et al*., 2015; 2017). For example, Grosse *et al*. (2015) proposed a conceptual framework that considers human factors in four critical categories (namely the "perceptual, mental, physical and psychosocial"). The authors suggested that the human factors can be incorporated into the planning models to improve the performance of order picking systems. More recently, Glock *et al*. (2019a) proposed an integrated model to determine the processing sequence for orders, pallet rotation, and picker routing to minimize

total picking effort. The authors considered the spinal loads on pickers and consequent risks of injury. Similar efforts had been made previously (Larco *et al*., 2017; Glock *et al*., 2019b).

Despite the fact that the idea of integrating human factors into order picking decision support systems is promising and necessary for human wellbeing, the above-cited order picking literature on human factors is concerned mostly with manual order picking (picker-to-parts order picking), rather than parts-to-picker order picking systems, which are the focus of our study. A parts-to-picker order picking system has the following operational features that differentiate it from a traditional picker-to-parts order picking system, which relies mainly on manpower.

First, a parts-to-picker ordering picking system relies substantially on the coordination between pickers and robots, to fulfill customer orders. Mobile robots lift racks that store SKUs and transport them from the storage area to stationary pickers to facilitate subsequent picking and packaging tasks by those pickers. In such parts-to-picker picking environments, robots must move forward and backward between the storage area and stationary pickers, forming closed loops between the storage area and the locations of the coordinated pickers. Accordingly, the efficiency of order fulfillment in a parts-to-picker picking system is contingent jointly upon the coordination between robots and pickers in carrying out the two consecutive tasks of handling racks (by mobile robots) and packaging (by pickers). Nevertheless, human-robot coordination often generates coordinating complexity and uncertainty as a result of the difficulty of sharing information, communication, and mutual adaption by the coordinated dyad (Faraj and Xiao, 2006).

Second, from a managerial perspective, an environment that includes working robots/machines is likely to differ from one that includes only human labors. Psychological effects (*e.g*., stress and strains) have attracted attention since computer-integrated/computer-aided/robot-aided manufacturing technologies were introduced for factory automation (Rosenthal, 1984; Karuppan and Schniederjans, 1995). As argued in Rosenthal (1984), the most difficult problems in automating a factory are managerial rather than technical. Olsen and Tomlin (2020) further highlighted the issue of managing worker-machine interfaces when robotics and artificial intelligence were introduced to convert manual operations into lean, digitized, and highly automated operations. Therefore, the issues that are raised by working with robots/machines seem not to be limited to those around technology and productivity. Instead, in the post-automation era, new psychological (Karuppan and Schniederjans, 1995), behavioral (Hinds, 2004), and organizational behavioral (Barrett *et al.*, 2012; Beane and Orlikowski, 2015) issues should be crucial for operations managers.

Considering the above research gaps in the literature on parts-to-picker order fulfillment and intralogistics operations, this work contributes to the field of intelligent logistics in the following three ways.

First, motivated by the sociotechnical theory (Cooper and Foster, 1971; Mumford, 2006), this work urges that the harmony of interrelations between human workers and robots in a parts-to-picker order fulfillment center should be considered in realizing intelligent logistics systems. In particular, this work promotes the development of adaptive human-friendly robotics to assist pickers in fulfilling orders with the fewest human-robot coordination conflicts. On the way toward “perfect automation”, the coexistence of robots and humans in

task environments is inevitable, requiring carefully planned mechanisms for agile robot-human coordination that are humanity-oriented and machine-assisted.

Second, the proposed methodology is novel in conceptualizing the aforementioned philosophy of machine-assisted humanity orientation into modeling and analysis to address the issue of robot-human coordination for parts-to-picker order fulfillment systems. Methodologically, this work integrates a discrete-time nonlinear dynamic stochastic model with a time-varying fatigue accumulation function to characterize and estimate a human picker's fatigue-dependent working states. Then, this work develops a stochastic optimal control-based data-driven solution approach, which permits not only estimating human pickers' instantaneous performance and robot queue lengths but also feeding back the aforementioned human picker's fatigue-dependent working states in real time to the coordinated robots to adjust their efficiencies in handling and distributing mobile racks to the picker. Such a real-time data-driven stochastic optimal control-based approach has its unique features and relative merits in addressing the critical yet under-explored issue on real-time robot-human coordination for machine-assisted order fulfillment systems.

Third, this work is innovative in the realization of ideas from occupational psychology (psychology), organizational behavior (sociology) and robotics (engineering) to address picker-robot coordination for intelligent logistics in contemporary operations (management). Psychological factors are considered in the development of a novel robot-human coordinated mechanism for use in an automated parts-to-picker order fulfillment system. Through normative analysis and real-data based empirical studies, the above concept (*i.e.*, machine-assisted humanity orientation) and proposed robot-picker coordinated order fulfillment mechanism are confirmed to be theoretically reasonable, and demonstrated to be of practical value in resolving the issue of interest.

3. PROBLEM DESCRIPTION

Typically, with our discussion with managers from a well-established e-commerce company in China and referring to the problem settings of Wang *et al*. (2022), the workflow of mobile robot-based parts-to-picker order fulfillment operations investigated in this paper contains the following steps. First, SKUs are received in the receiving area of a warehouse/distribution center; meanwhile, mobile robots that carry empty racks are dispatched to load the received SKUs. This is followed by the step of storage assignment, where mobile robots move loaded racks to the storage area (Li *et al*., 2020). If the SKUs in the racks are required in an order processing list, then the mobile robots move the racks with those required SKUs from the storage area to the picking-packaging area (termed as the step of rack handling and distribution). Then, stationary pickers in the picking-packaging area pick out the SKUs that are identified in the picking list, and package them into cardboard boxes to fulfill customer orders (termed as the step of picking and packaging). This step is followed by automatically moving the completed cardboard boxes by means of conveyers to the outbound area for vehicular loading and dispatching. Mobile robots that have completed the delivery of the racks with the required SKUs to the stationary pickers return from the picking area to the storage area for repeated execution of the step of rack

handling and distribution to facilitate pickers' carrying out picking and packaging for order fulfillment. Similar mobile robot-based parts-to-picker order fulfillment operations can also be readily found in numerous practical cases, including in Amazon.com (Demaitre, 2019; Gharehgozli and Zaerpour. 2020; Garland , 2022).

This work focuses on coordinating the step of rack handling and distribution (executed by robots) and the step of picking and packaging (executed by pickers). Specifically, the performance of mobile robots in handling and moving racks (number of racks handled and moved per robot per time unit) significantly influences the associated picker's performance in the subsequent picking and packaging tasks. The effect of psychological and behavioral uncertainties, which may be evident in the interaction between pickers and robots, on an associated picker's performance is considered herein. Accordingly, the problem of interest and goals of this work are as follows.

Consider a few-to-one parts-to-picker picking system, in which a few mobile robots work collaboratively with a human picker. A set of C customer orders, involving S SKUs, and being stored in N racks must be handled and moved by M mobile robots from the storage area to the picking area. Then, they have to be picked and packaged by one associated picker in a given working period T (*e.g.*, 3 hours) without the intervention of scheduled breaks. A shared storage (scattered storage) policy, which is typically applied to mobile robot-based parts-to-picker picking systems (Weidinger *et al*., 2018), is adopted. Different SKUs may be stored in a rack, and each rack can be associated with one or more customer orders. Two goals must be achieved. The first is to complete picking and packaging of the aforementioned S SKUs that are stored and scattered over R racks by smoothly coordinating the operations of M mobile robots and the associated picker during a working period T . This goal must be achieved under the condition that the picker's fatigue increment ($\Delta\rho_k$) in any time interval k ($k=\{1,2,3...K\}; T=K\cdot\bar{t}$) during T should not exceed a predetermined fatigue degree ($\bar{\rho}$), such that the accumulated fatigue degree (ρ_K) in the last time interval K does not exceed its upper bound (ρ_{max}), where $\bar{t}$ is the length of a time interval. Meanwhile, in the few-to-one parts-to-picker picking system, the second goal is that the processed racks in the picking area are efficiently returned to the storage area by mobile robots for the next round of order processing.

Based on the above problem description and defined goals, this work proposes a real-time robot-picker coordinated order fulfillment system that comprises the following four subsystems: (1) robot-based rack handling (*Subsystem* 1), (2) mobile robot-carried rack movement (*Subsystem* 2), (3) human-based picking and packaging (*Subsystem* 3), and (4) robot-based rack return (*Subsystem* 4), which are depicted in Fig. 1. The number of newly arriving (A_k) racks that are loaded with SKUs from the receiving area to storage area is treated as an exogenous variable, which is given in each time interval k ($\forall k$). *Subsystems* 2 and 4 are virtual as they are specified to determine the time-varying distribution rates (μ_k and ν_k) of forward and reverse logistics for mobile racks that move between the storage (*Subsystem* 1) and picking-packaging (*Subsystem* 3) areas in any time interval k ($\forall k$). *Subsystems* 1 and 3 correspond to task operations that are executed by robots and associated pickers in the storage and picking-packaging areas, respectively. The outputs of *Subsystems* 1 and 3

are the number of racks (X_k) that are handled by mobile robots and the number of racks (Y_k) that are processed by a picker in each time interval k ($\forall k$). Both X_k and Y_k can be treated as metrics that are evaluated by contemporary detection technologies, such as image processing-based detectors.

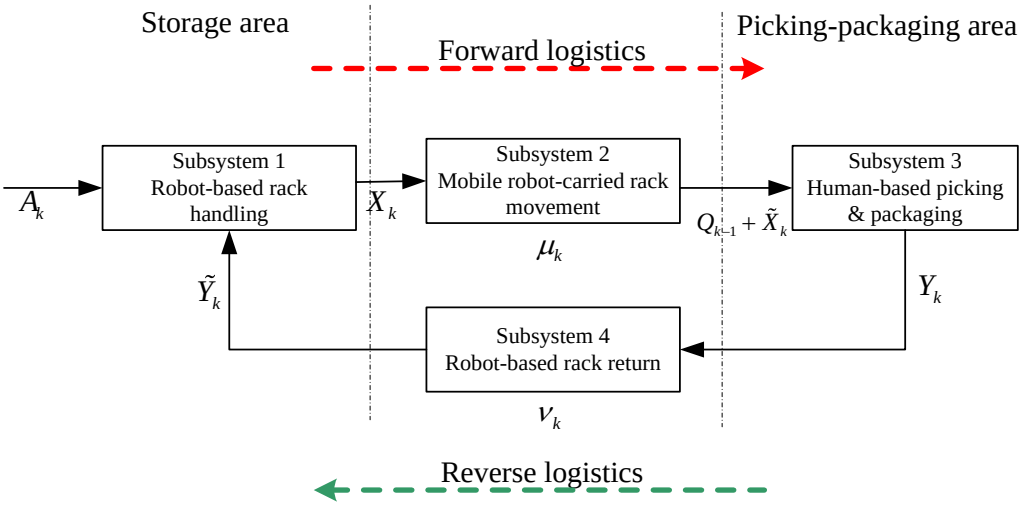

Fig. 1. The proposed real-time robot-picker coordinated order fulfillment system.

The proposed robot-picker coordinated order fulfillment system has three distinctive features. First, the rack-based order processing cycle, which integrates the forward and reverse logistical flows of mobile racks between the storage and picking-packaging areas, is considered. A closed-loop rack reuse process facilitates the corresponding logistical resource management in the system. Second, the interactions between robots and associated pickers are considered, and they are characterized by the instantaneous inputs (Q_k and $Q_{k|k}$) , which are defined as the perceived queue lengths of unprocessed racks at the beginning and end of time interval *k*, respectively, and output (Y_k , which is the number of racks that are processed by a picker in time interval *k*). Q_k and $Q_{k|k}$ are given by

$$\begin{cases} Q_k = Q_{k-1|k-1} + \tilde{X}_k \\ Q_{k|k} = Q_k - Y_k \end{cases}, \ \forall k, \tag{1}$$

where $Q_{k-1|k-1}$ ($Q_{k-1|k-1} = Q_{k-1} - Y_{k-1}$) represents the number of unprocessed racks in the queue in the picking-packaging area (*Subsystem* 3) at the end of time interval $k-1$; and $\tilde{X}_k$ represents the number of unprocessed racks that arrive at the picking-packaging area (*Subsystem* 3) in time interval *k*. Third, the picker's psychological and physical conditions, characterized by the accumulated fatigue degree (ρ_k) and its association with Y_k and Q_k , are considered, and fed back to adjust the handling, transportation, and return decisions of the robots that are executed in *Subsystems* 1, 2, and 4, respectively. Hence, the picking and packaging tasks can be completed in a manner that includes critical human factors.

4. MODELING

This section proposes a discrete-time nonlinear dynamic stochastic model to formulate and solve the above problem. Specifically, subsection 4.1 defines the variables of system states (including state variables and control variables) and subsection 4.2 explicates the proposed dynamic stochastic model.

4.1. Specification of System States

The state variables of *Subsystem* 3 are specified to define the expected performance of a picker in coordination with mobile robots. Then, the state variables for *Subsystem* 1 are specified to characterize the performance of the coordinated robots. Thereafter, the state variables of *Subsystems* 2 and 4 are specified to characterize the forward and reverse logistical flows of mobile racks that are required for coordination between Subsystems 1 and 3 (robots' and human pickers' actions).

4.1.1. States of human picker

Consider the states that are ideally associated with a picker's performance (*Subsystem* 3). Ideally, the picking and packaging tasks of a picker are carried out efficiently by seamlessly receiving and processing the loaded racks that are delivered by mobile robots. However, such an ideal state of *Subsystem* 3 is obtained at the cost of the picker's accumulated fatigue (ρ_k). Worker fatigue is multidimensional, and often increases with time (Jaber *et al*., 2013; Glock *et al.*, 2019b), stress and workload (MacDonald, 2003; Kc and Terwiesch, 2009; Do *et al*., 2018), particularly when a picker must perform repetitive picking and packaging tasks. Based on the learning-forgetting-fatigue–recovery models established in the ergonomics-related literature (Jaber *et al*. 2013; Glock *et al.*, 2019b), the commonly used deterministic exponential form of accumulated fatigue is extended herein into a dynamic stochastic form. Specifically, the fatigue growth rate (λ_k) that determines the speed of fatigue accumulation is associated with the perceived queue length of unprocessed racks (Q_k) and work rate (Y_k). Therein, Q_k and Y_k can be treated, respectively, as the instantaneous mental and physical workloads which have been empirically verified to have adverse impact on fatigue (Tan and Netessine, 2014). This work utilizes Q_k and Y_k to capture how both the instantaneous mental and physical workloads affect a picker's accumulated fatigue in any given time interval k ($\forall k$). Thus, the picker's accumulated fatigue (ρ_k) in time interval k ($\forall k$) varies with time, and can be expressed in a recursive form given by

$$\rho_k = \rho_{k-1} + \Delta\rho_k, \forall k, \tag{2}$$

where ρ_{k-1} is the picker's accumulated fatigue in time interval $k-1$, and $\Delta\rho_k$ represents the fatigue increment in time interval k and equals $1-e^{-\lambda_k}$ ($\Delta\rho_k = 1-e^{-\lambda_k}$). According to the empirical results of MacDonald (2003) from multiple regression analyses, both workloads (Q_k) and work rates (Y_k) have amplified impact on fatigue, inferring that λ_k can be characterized by Q_k and Y_k in a simple linear manner as

$$\lambda_k = \beta_0 + \beta_1 Y_k + \beta_2 Q_k, \forall k, \quad (3)$$

where β_0 ($\beta_0 \geq 0$) is the intrinsic fatigue growth rate; β_1 ($\beta_1 \geq 0$) and β_2 ($\beta_2 \geq 0$) are the coefficients that capture the associations of Y_k and Q_k with λ_k, respectively. The following condition on the picker's fatigue that accumulates in any time interval (Eq. (4)) must hold to ensure the well-being of the human worker).

$$\rho_k \leq \rho_{\max}, \forall k, \quad (4)$$

The accumulated fatigue (ρ_k) in time interval k may have a negative ergonomic effect on a picker's work rate (Y_{k+1}) in the next time interval $k+1$ (MacDonald, 2003; Jaber *et al*. 2013): a higher ρ_k often corresponds to a lower Y_{k+1}. Similarly, as shown by Kc and Terwiesch (2009), the overwork that is associated with accumulated fatigue has been demonstrated to affect a worker's performance (*e.g.*, service rate). Do *et al*. (2018) assumed that the service rate has a multiplicative form under the effect of overwork. With reference to the fatigue-recovery model of Jaber *et al*. (2013) and the above literature, in this work, a simple negative exponential function ($f(\rho_k)$, $f(\rho_k) \equiv e^{-\rho_k}$) is used to capture the moderating effect of ρ_k, which can be expressed in a simple multiplicative form as shown in Eq. (5).

$$Y_{k+1} = f(\rho_k) Y_k = e^{-\rho_k} Y_k, \forall k, \quad (5)$$

Accordingly, Eq. (5) can be used to elucidate how the accumulated fatigue in any given time interval k influences a picker's instantaneous picking and packaging performance in the next time interval $k+1$. Moreover, the system states and control variables of robots in response to a picker's fatigue-dependent performance can also be determined.

In addition to the above concern about accumulated fatigue, the efficiency of picking and packaging tasks in each time interval is an important issue. Ideally, a picker processes all loaded racks as they arrive to the picking-packaging area from the storage area so that no racks remain in a queue in any time interval ($Q_k = Y_k$, $\forall k$). Let γ_k be the picker-efficiency state, which is defined as $\gamma_k \equiv \frac{Y_k}{Q_k} = \frac{Y_k}{Q_{k-1} + \tilde{X}_k}$ (Eq. (1)), and $\bar{\gamma}$ ($\bar{\gamma}$=1 , $\forall k$) be the ideal state of γ_k. Then, γ_k is expected to remain stable in each time interval ($\gamma_{k+1} = \gamma_k$, $\forall k$) under the ideal condition. If it does so, then $\gamma_{k+1} = \gamma_k = \bar{\gamma} = 1$ in all time intervals ($\forall k$), including the initial time interval ($k = 0$). In practice, γ_k may change over time and exhibit stochastic features under the influence of other system states (*e.g.*, accumulated fatigue ρ_k) and exogenous variables (*e.g.*, A_k, $\forall k$). According to Eq. (5), Y_{k+1} which is one component of γ_{k+1}, can be influenced by $f(\rho_k)$ owing to the moderating effect of accumulated fatigue. Given Q_k and $\tilde{X}_{k+1}$, which are exogenous variables to this subsystem (*Subsystem* 3), γ_{k+1} can be associated with γ_k in a simple deterministic form as $\gamma_{k+1} = e^{-\rho_k} \gamma_k$ to indicate the effect of accumulated fatigue on worker performance (Jaber *et al*., 2013). If the stochastic features of the state variables

are further considered, the above deterministic form can be extended into a recursive form with a Gaussian white noise term (w_{γ_k}), as shown in Eq. (6), to capture its dynamic and stochastic features.

$$\begin{cases} \gamma_{k+1} = e^{-\rho_k}\gamma_k + w_{\gamma_k} & , \forall k\ (k>0), \\ \gamma_0 = \overline{\gamma} = 1 \end{cases} \tag{6}$$

where w_{γ_k} is a Gaussian white noise term of γ_k. Then, the ideal state of γ_k ($\overline{\gamma}$) is $\overline{\gamma}=1$ ($\forall k$), which means that no racks are queuing in the picking-packaging area in any time interval.

4.1.2. States of mobile robots

In the ideal state, robots handle SKUs and racks in the storage area (*Subsystem* 1) in a way that maintains equal volumes of inbound and outbound rack flows of *Subsystem* 1 ($X_k = A_k + \tilde{Y}_k$, $\forall k$). Let δ_k be the robot-efficiency rate, which is defined as $\delta_k \equiv \frac{X_k}{A_k + \tilde{Y}_k}$, and $\overline{\delta}$ ($\overline{\delta}=1$, $\forall k$) be the ideal state of δ_k. Then, δ_k should remain the same in all time intervals under the ideal condition, such that $\delta_{k+1} = \delta_k = \overline{\delta} = 1$ ($\forall k$). Despite the fact that fatigue accumulation does not apply to *Subsystem* 1, involving robots' operations, a robot-efficiency state (δ_k) can be influenced by the exogenous variables (*e.g.*, A_k, $\forall k$) and $\tilde{Y}_k$ which is contingent upon the picker's performance. Like γ_k, δ_k has dynamic and stochastic features. Thus, δ_k can be expressed in the recursive form with a Gaussian white noise term (w_{δ_k}) as follows

$$\begin{cases} \delta_{k+1} = \delta_k + w_{\delta_k} & , \forall k\ (k>0), \\ \delta_0 = \overline{\delta} = 1. \end{cases} \tag{7}$$[4]

4.1.3. Control variables for forward and reverse logistics flows of racks

Subsystems 2 and 4 are designed to regulate the forward and reverse logistical distribution flows of racks between the storage area and picking-packaging area. Let μ_k and ν_k be the rack distribution rates that are associated with *Subsystems* 2 and 4 (Fig. 1) and defined as $\mu_k \equiv \frac{\tilde{X}_k}{X_k}$ and $\nu_k \equiv \frac{\tilde{Y}_k}{Y_k}$, respectively. Then, μ_k and ν_k can be used as control variables to regulate the numbers of unprocessed ($\tilde{X}_k$) and processed ($\tilde{Y}_k$) racks that arrive at *Subsystem* 3 and *Subsystem* 1 in each given time interval k by setting $\tilde{X}_k = u_k X_k$ and $\tilde{Y}_k = \nu_k Y_k$, respectively, such that the system states (γ_k and δ_k) that are associated with the human picker and robots become

$$\gamma_k = \frac{Y_k}{Q_{k-1} + \mu_k X_k}, \forall k, \tag{8}$$

[4] We let δ_0 (initial value of δ) start from the ideal value, meaning that its initial state starts from an ideal condition.

$$\delta_k = \frac{X_k}{A_k + \nu_k Y_k}, \forall k. \tag{9}$$

Based on the above efficiency-related states (γ_k and δ_k) and control variables (μ_k and ν_k) defined above, and given the number of newly arriving racks (A_k) and the measured previous queue length of racks (Q_{k-1}), the following analytical results (Theorem 4.1) regarding the outputs $\hat{X}_k$ and $\hat{Y}_k$ (estimates of instantaneous efficiency rates associated with coordinated robots and picker) from *Subsystems* 1 and 3, respectively, can be derived . Note that all technical proofs are provided in *Online Appendix A*.

Theorem 4.1. *Given* γ_k, δ_k, μ_k, ν_k, A_k, Q_{k-1} *and* $\mathbf{\Omega}_k \equiv \delta_k \mu_k \nu_k \gamma_k$, *the estimates of instantaneous projections of* X_k *and* Y_k *(denoted by* $\hat{X}_k$ *and* $\hat{Y}_k$ *are obtained as*

$$\hat{X}_k = \frac{1}{1-\mathbf{\Omega}_k}\left(\delta_k A_k + \frac{\mathbf{\Omega}_k Q_{k-1}}{\mu_k}\right), \forall k, \tag{10}$$

$$\hat{Y}_k = \frac{1}{1-\mathbf{\Omega}_k}\left(\frac{\mathbf{\Omega}_k A_k}{\nu_k} + \gamma_k Q_{k-1}\right), \forall k. \tag{11}$$

In Eqs. (10) and (11) of Theorem 4.1, $\mathbf{\Omega}_k$ is the product of the subsystem states (γ_k, δ_k) and control variables (μ_k, ν_k); A_k can be treated as an exogenous variable of the system; and Q_{k-1} refers to queuing racks in the previous time interval $k-1$. Both A_k and Q_{k-1} are predetermined; however, γ_k, δ_k, μ_k, and ν_k ($\forall k$) are unknown, and must be estimated (as detailed in the next subsection (4.2)).

Based on Theorem 4.1, Corollary 4.1 is also used to characterize and estimate the time-varying fatigue growth rate (λ_k) and fatigue increment ($\Delta\rho_k$) in any time interval k ($\forall k$).

Corollary 4.1. *Given Theorem 4.1, estimates of* λ_k *and* $\Delta\rho_k$ *(denoted by* $\hat{\lambda}_k$ *and* $\Delta\hat{\rho}_k$*) are obtained as*

$$\hat{\lambda}_k = \beta_0 + (\beta_1 \gamma_k + \beta_2)\left(\frac{\delta_k \mu_k A_k + Q_{k-1}}{1-\mathbf{\Omega}_k}\right), \forall k, \tag{12}$$

$$\Delta\hat{\rho}_k = 1 - e^{-\left(\beta_0 + (\beta_1\gamma_k + \beta_2)\left(\frac{\delta_k \mu_k A_k + Q_{k-1}}{1-\mathbf{\Omega}_k}\right)\right)}, \forall k, \tag{13}$$

Based on Corollary 4.1, substituting Eq. (13) into Eq. (2) yields

$$\rho_k = \rho_{k-1} + 1 - e^{-\left(\beta_0 + (\beta_1\gamma_k + \beta_2)\left(\frac{\delta_k \mu_k A_k + Q_{k-1}}{1-\mathbf{\Omega}_k}\right)\right)}, \forall k. \tag{14}$$

Using the correlations between the system states and control variables specified above, the human picker and robots can be readily coordinated for superior performance in an order fulfillment center once the optimal values of the state and control variables can be determined. It is noted that the proposed model is data-driven in which the input data required (including Y_k and A_k) are collected in each time interval k ($\forall k$) for

estimating efficiency-related states (γ_k and δ_k) and control variables (μ_k and ν_k) in each time interval k ($\forall k$) such that the state variables (γ_k and δ_k) can move toward the associated ideal values. Therein, the data used are collected in each time interval, which is expressed in a discrete-time manner rather than a continuous time manner for dynamically estimating and controlling state variables. Thus, the problem is formulated in a discrete-time rather than a continuous-time manner, as presented in the next subsection (4.2).

4.2. Model

This subsection proposes a discrete-time nonlinear dynamic stochastic model which is characterized by recursive and measurement equations subject to boundary constraints (Santina *et al*., 1994; Sheu, 2002; Anderson, Jr. *et al*., 2006). Specifically, the time-varying relationships among state variables, control variables, and measurement data defined in the previous section (Section 3), can be characterized in three forms: (1) recursive equations, (2) measurement equations, and (3) boundary constraints, as follows.

The recursive equations specify time-varying relationships between the states of a dynamic and stochastic system in the next and current time intervals ($k+1$ and k, $\forall k$). Among such system states, γ_k, and δ_k are treated as independent states, whereas ρ_k is a state that depends on γ_k and δ_k, according to Corollary 4.1 and Eq. (14). In the proposed model, only the time-varying relationships of independent states (γ_k, and δ_k) must be formulated recursively; then, the dependent state ρ_k can be readily determined. Based on Eqs. (6) and (7), the recursive equations that are associated with γ_k and δ_k can expressed in a generalized vector form as in Eq. (15).

$$\mathbf{\Phi}_{k+1} = \mathbf{F}_k + \mathbf{W}_k, \forall k, \tag{15}$$

where $\mathbf{\Phi}_{k+1}$, $\mathbf{F}_k$ and $\mathbf{W}_k$ are 2×1 time-varying state vectors, and can be further expressed as

$$\mathbf{\Phi}_{k+1} = \begin{bmatrix} \gamma_{k+1} \\ \delta_{k+1} \end{bmatrix}, \forall k, \tag{16}$$

$$\mathbf{F}_k = \begin{bmatrix} e^{-\rho_k}\gamma_k \\ \delta_k \end{bmatrix}, \forall k, \tag{17}$$

$$\mathbf{W}_k = \begin{bmatrix} w_{\gamma_k} \\ w_{\delta_k} \end{bmatrix}, \forall k, \tag{18}$$

where $\rho_k = \rho_{k-1} + 1 - e^{-\left(\beta_0 + (\beta_1\gamma_k + \beta_2)\left(\frac{\delta_k \mu_k A_k + Q_{k-1}}{1-\mathbf{\Omega}_k}\right)\right)}$, as in Eq. (14) of Corollary 4.1.

Accordingly, the recursive equations (Eqs. (15)-(18)) reveal that the system states γ_k and δ_k change over time, following the standard Gaussian-Markov processes and can be used to project γ_{k+1}, and δ_{k+1} one time interval ahead, based on γ_k and δ_k in any time interval k ($\forall k$).

The measurement equations characterize time-varying relationships between measurements and system states. In this work, Y_k (the number of mobile racks that are processed by a picker in each given time interval k) is used as the measurement variable because it can be detected/measured readily using various detection technologies (such as image processing and automated counters). Based on Eq. (11) in Theorem 4.1, we can further postulate the deterministic form of time-varying relationships between the measurement (Y_k) and system states as $Y_k = \frac{1}{1-\mathbf{\Omega}_k}\left(\frac{\mathbf{\Omega}_k A_k}{\nu_k} + \gamma_k Q_{k-1}\right)$. Owing to the measurement error in Y_k in any given time interval k ($\forall k$), a Gaussian white noise term ε_k is used to characterize this property. Since only one measurement variable (Y_k) is involved, one measurement equation is associated with Y_k in the proposed model. The generalized form of the measurement equation is given by

$$\mathbf{Y}_k = \mathbf{H}_k + \boldsymbol{\varepsilon}_k, \forall k, \tag{19}$$

where $\mathbf{Y}_k$, $\mathbf{H}_k$ and $\boldsymbol{\varepsilon}_k$ are 1×1 time-varying state vectors, which can be further expressed as

$$\mathbf{Y}_k = Y_k, \forall k, \tag{20}$$

$$\mathbf{H}_k = \left[\frac{1}{1-\mathbf{\Omega}_k}\left(\frac{\mathbf{\Omega}_k A_k}{\nu_k} + \gamma_k Q_{k-1}\right)\right], \forall k, \tag{21}$$

$$\boldsymbol{\varepsilon}_k = \varepsilon_k, \forall k. \tag{22}$$

Additionally, the picker's accumulated fatigue ($\rho_k, \forall k$) in any time interval should not exceed a preset upper bound ($\rho_{\max}$), as indicated in Eq. (4). This constraint is incorporated into the proposed model.

5. REAL-TIME DATA-DRIVEN STATE ESTIMATION

This section presents a stochastic optimal control-based method for the real-time estimation of system states (γ_k and δ_k) and control variables (μ_k and ν_k), given information about the number of newly arriving racks (A_k) and the number of racks processed by the picker, Y_k, in each time interval ($\forall k$). Based on the principles of optimality that are applied in stochastic optimal control theory (Santina *et al.*, 1994), the proposed algorithm searches for the optimal solutions for γ_k, δ_k, μ_k and ν_k which are updated using measurements of Y_k and the measurement equation (Eq. (19)) in each time interval k ($\forall k$), and then fed back as inputs into the recursive equation (Eq. (15)) such that the objective function ξ (Eq. (23)) is minimized.

$$\xi = \min\ E\left\{\sum_{k=1}^{K}\left(\hat{\mathbf{\Phi}}_k - \mathbf{\Phi}_k^*\right)^{\mathrm{T}} \mathbf{\Psi}_k^{\Phi}\left(\hat{\mathbf{\Phi}}_k - \mathbf{\Phi}_k^*\right) + \left(\hat{\mathbf{U}}_k - \mathbf{U}_k^*\right)^{\mathrm{T}} \mathbf{\Psi}_k^{\mathrm{U}}\left(\hat{\mathbf{U}}_k - \mathbf{U}_k^*\right)\right\}, \tag{23}$$

where $\hat{\mathbf{\Phi}}_k$ and $\hat{\mathbf{U}}_k$ are 2×1 vectors that contain the estimated system states (γ_k and δ_k) and estimated control variables (μ_k and ν_k) in time interval k, respectively; $\mathbf{\Phi}_k^*$ and $\mathbf{U}_k^*$ are 2×1 vectors that contain the ideal values of system states and control variables that are associated with $\hat{\mathbf{\Phi}}_k$ and $\hat{\mathbf{U}}_k$, respectively; and $\mathbf{\Psi}_k^{\Phi}$ and $\mathbf{\Psi}_k^{U}$ represent 2×2 time-varying diagonal, positive-definite weighting matrixes that are associated with $\hat{\mathbf{\Phi}}_k$ and $\hat{\mathbf{U}}_k$, respectively. The objective function ξ in Eq. (23) is the cost function, which is a scalar quadratic performance measure that indicates the deviation of the estimated system states and control variables from their ideal values in the order processing period.

To estimate the aforementioned system states and control variables in real time, a stochastic optimal control-based method is developed using an extended Kalman filter. Kalman filtering is a well-known statistical method for the linear-quadratic estimation of system states of dynamic and stochastic systems. It has been successfully and extensively utilized in solving diverse estimation and control problems in various fields, such as the tracking and navigation of different sorts of vehicles, and traffic signal control (Sheu, 2002). Whereas the basic Kalman filter applies to linear problems, the extended Kalman filter has been developed particularly for nonlinear problems that are characterized by either recursive or measurement equations in dynamic and stochastic models (Santina *et al.*, 1994). The primary computational steps in the proposed estimation method are summarized below.

5.1. Initialization

This step initializes system states and all of the inputs that are required to trigger the subsequent computational steps. Let $k=0$ and $\Delta\mathbf{\Phi}_k \equiv \mathbf{\Phi}_k - \hat{\mathbf{\Phi}}_k$ ($\forall k$). Then, preset the initial estimates of the 2×1 state vector ($\hat{\mathbf{\Phi}}_0$), the 2×1 control variable vector ($\hat{\mathbf{U}}_0$), the number of queued racks (Q_0), and the 2×2 covariance matrix of the state estimation error ($\hat{\mathbf{P}}_{0|0}$), where $Q_0=0$; $\hat{\mathbf{\Phi}}_0$, $\hat{\mathbf{U}}_0$ and $\hat{\mathbf{P}}_{0|0}$ are given by

$$\begin{cases} \hat{\mathbf{\Phi}}_0 \equiv \begin{bmatrix} \hat{\gamma}_0 \\ \hat{\delta}_0 \end{bmatrix} = \begin{bmatrix} \overline{\gamma} \\ \overline{\delta} \end{bmatrix} \\ \hat{\mathbf{U}}_0 \equiv \begin{bmatrix} \hat{\mu}_0 \\ \hat{\nu}_0 \end{bmatrix} = \begin{bmatrix} 1 \\ 1 \end{bmatrix} \end{cases} \quad \text{(when } k=0\text{)}, \tag{24}$$

$$\hat{\mathbf{P}}_{0|0} \equiv E\left[\Delta\mathbf{\Phi}_0 \Delta\mathbf{\Phi}_0{}^{\mathrm{T}}\right] = \mathbf{P}_0, \text{ (where } k=0\text{)}. \tag{25}$$

5.2. Prior Prediction of System states

In this step, the state vector $\mathbf{\Phi}_{k+1}$ and covariance matrix of the state estimation error $\mathbf{P}_{k+1}$ in time interval $k+1$ are predicted using the estimates of system states and measurements made in time interval k ($\forall k$). The prior prediction of $\mathbf{\Phi}_{k+1}$ ($\hat{\mathbf{\Phi}}_{k+1|k}$) will be updated for the linear minimum mean square (LMMS) estimation of $\mathbf{\Phi}_{k+1}$ using the extended Kalman filter in the next stage; and the prior prediction of $\mathbf{P}_{k+1}$ ($\hat{\mathbf{P}}_{k+1|k}$) is a prerequisite

for the aforementioned state estimation. Using Eq. (15), Corollary 5.1 and 5.2 are provided to facilitate the prior predictions of $\hat{\mathbf{\Phi}}_{k+1|k}$ and $\hat{\mathbf{P}}_{k+1|k}$, respectively.

Corollary 5.1. *Given Eq. (15) (recursive equation) and its characteristics, let* $\hat{\mathbf{F}}_k \equiv \begin{bmatrix} e^{-\hat{\rho}_k}\hat{\gamma}_k \\ \hat{\delta}_k \end{bmatrix}$, *where* $\hat{\gamma}_k$ *and* $\hat{\delta}_k$ *are the LMMS estimates of* γ_k *and* δ_k *that are based on the data regarding* A_k *and* Y_k *collected in time interval* k. *Then, the prior prediction of the LMMS estimate of* $\mathbf{\Phi}_{k+1}$ *(*$\hat{\mathbf{\Phi}}_{k+1|k}$*) that is based on the data regarding* A_k *and* Y_k *that were collected in time interval* k *is given by*

$$\hat{\mathbf{\Phi}}_{k+1|k} = \hat{\mathbf{F}}_k, \forall k, \tag{26}$$

The prior prediction ($\hat{\mathbf{P}}_{k+1|k}$) of the covariance matrix of the state estimation error $\mathbf{P}_{k+1}$ as well as $\hat{\mathbf{\Phi}}_{k+1|k}$ must be determined in this stage. Using Eq. (15) and Eq. (26) (Corollary 5.1), Corollary 5.2 is obtained to determine $\hat{\mathbf{P}}_{k+1|k}$.

Corollary 5.2. *Given Eq. (15) (the recursive equations) and Corollary 5.1, let* $\hat{\mathbf{F}}'_k = \left.\frac{\partial \mathbf{F}_k}{\partial \mathbf{\Phi}_k}\right|_{\mathbf{\Phi}_k = \hat{\mathbf{\Phi}}_k}$ *based on the data regarding* A_k *and* Y_k *that were collected in time interval k, and let* $\mathbf{R}_k \equiv E[\mathbf{W}_k \mathbf{W}_k^{\mathrm{T}}]$. *Then, the prior prediction of* $\mathbf{P}_{k+1}$ *(*$\hat{\mathbf{P}}_{k+1|k}$*) that is based on the data regarding* A_k *and* Y_k *that were collected in time interval k is given by*

$$\hat{\mathbf{P}}_{k+1|k} = \hat{\mathbf{F}}'_k \hat{\mathbf{P}}_{k|k} \hat{\mathbf{F}}'^{\mathrm{T}}_k + \mathbf{R}_k, \forall k. \tag{27}$$

5.3. Correction of Prior Predictions

In this stage, the prior predictions $\hat{\mathbf{\Phi}}_{k+1|k}$ and $\hat{\mathbf{P}}_{k+1|k}$ are corrected using the Kalman gain ($\mathbf{G}_{k+1}$) and the measurements made through time interval $k+1$ ($\forall k$). To achieve this purpose, Corollary 5.3, which associates the corrected state vector ($\hat{\mathbf{\Phi}}_{k+1}$) with its prior prediction ($\hat{\mathbf{\Phi}}_{k+1|k}$), the Kalman gain ($\mathbf{G}_{k+1}$) and the measurements made through time interval $k+1$ ($\forall k$), is provided.

Corollary 5.3. *Given Eqs. (5) (fatigue prediction function) and (19) (measurement equation), let* $\Delta\mathbf{y}_{k+1|k}$ *be the measurement residual in time interval* $k+1$, *defined as* $\Delta\mathbf{y}_{k+1|k} \equiv \mathbf{Y}_{k+1} - \hat{\mathbf{Y}}_{k+1|k} = \mathbf{Y}_{k+1} - e^{-\hat{\rho}_k}\hat{\mathbf{H}}_k$ *(*$\forall k$*),* *where* $\hat{\mathbf{H}}_k = \left[\frac{1}{1-\hat{\mathbf{\Omega}}_k}\left(\frac{\hat{\mathbf{\Omega}}_k A_k}{\hat{v}_k} + \hat{\gamma}_k Q_{k-1}\right)\right]$ *(by Eq. (21)), and let* $\Delta\mathbf{Y}_k$ *be a* $k \times 1$ *residual vector of the*

measurement residuals through time interval k *that is defined as* $\Delta\mathbf{Y}_k \equiv \begin{bmatrix} \Delta\mathbf{y}_{1|0} \\ \Delta\mathbf{y}_{2|1} \\ \vdots \\ \Delta\mathbf{y}_{k|k-1} \end{bmatrix}$. *Then, the LMMS estimate of* $\mathbf{\Phi}_{k+1}$ *(*$\hat{\mathbf{\Phi}}_{k+1}$*) that is based on the data that were collected through time interval* $k+1$ *is given by*

$$\hat{\mathbf{\Phi}}_{k+1} = \hat{\mathbf{\Phi}}_{k+1|k} + \mathbf{G}_{k+1} \cdot \Delta\mathbf{y}_{k+1|k} + \mathbf{m}_{\mathbf{\Phi}}, \forall k, \tag{28}$$

where $\mathbf{m}_{\mathbf{\Phi}}$ *is the mean of* $\mathbf{\Phi}_{k+1}$*, and* $\mathbf{G}_{k+1}$ *is the Kalman gain, which is defined as*

$$\mathbf{G}_{k+1} \equiv E[\mathbf{\Phi}_{k+1}\Delta\mathbf{y}_{k+1|k}^{\mathrm{T}}] \cdot \{E[\Delta\mathbf{y}_{k+1|k}\Delta\mathbf{y}_{k+1|k}^{\mathrm{T}}]\}^{-1}, \forall k. \tag{29}$$

As seen in Eqs. (28) and (29) of Corollary 5.3, the LMMS estimate of $\mathbf{\Phi}_{k+1}$ ($\hat{\mathbf{\Phi}}_{k+1}$) given the measurements made through time interval $k+1$ can be derived following the determination of the Kalman gain $\mathbf{G}_{k+1}$ as in Eq. (29). Therefore, Corollary 5.4 is provided to determine the Kalman gain $\mathbf{G}_{k+1}$.

Corollary 5.4. *Given Corollaries 5.2 and 5.3, and Eq. (19) (measurement equation), let* $\hat{\mathbf{H}}'_{k+1} = \left.\dfrac{\partial\mathbf{H}_{k+1}}{\partial\mathbf{\Phi}_{k+1}}\right|_{\mathbf{\Phi}_{k+1}=\hat{\mathbf{\Phi}}_{k+1|k}}$ *and* $\mathbf{\Lambda}_{k+1} \equiv E[\boldsymbol{\varepsilon}_k\boldsymbol{\varepsilon}_k{}^{\mathrm{T}}]$. *Then, the Kalman gain* $\mathbf{G}_{k+1}$ *is given by*

$$\mathbf{G}_{k+1} = \hat{\mathbf{P}}_{k+1|k}\hat{\mathbf{H}}'^{\mathrm{T}}_{k+1}(\hat{\mathbf{H}}'_{k+1}\hat{\mathbf{P}}_{k+1|k}\hat{\mathbf{H}}'^{\mathrm{T}}_{k+1} + \mathbf{\Lambda}_{k+1})^{-1}, \forall k. \tag{30}$$

Based on Corollaries 5.3 and 5.4, the corrected state vector $\hat{\mathbf{\Phi}}_{k+1}$ can be obtained using Eqs. (28) and (30). Alternatively, $\hat{\mathbf{\Phi}}_{k+1}$ can also be expressed as

$$\hat{\mathbf{\Phi}}_{k+1} = \hat{\mathbf{\Phi}}_{k+1|k} + \hat{\mathbf{P}}_{k+1|k}\hat{\mathbf{H}}'^{\mathrm{T}}_{k+1}(\hat{\mathbf{H}}'_{k+1}\hat{\mathbf{P}}_{k+1|k}\hat{\mathbf{H}}'^{\mathrm{T}}_{k+1} + \mathbf{\Lambda}_{k+1})^{-1} \cdot \Delta\mathbf{y}_{k+1|k} + \mathbf{m}_{\mathbf{\Phi}}, \forall k. \tag{31}$$

Finally, the recursive equation for correcting the prior prediction of the covariance matrix of state estimation error $\hat{\mathbf{P}}_{k+1|k}$ into $\hat{\mathbf{P}}_{k+1|k+1}$ must be derived for the recursive estimation of system states in the next time interval $k+1$. To achieve this purpose, Corollary 5.5 is provided.

Corollary 5.5. *Given Corollaries 5.2 to 5.4, let the corrected covariance matrix of state estimation error* $\hat{\mathbf{P}}_{k+1|k+1}$ *be defined as* $\hat{\mathbf{P}}_{k+1|k+1} \equiv E[\Delta\mathbf{\Phi}_{k+1|k+1}\Delta\mathbf{\Phi}^{\mathrm{T}}_{k+1|k+1}]$*, where* $\Delta\mathbf{\Phi}_{k+1|k+1} \equiv \mathbf{\Phi}_{k+1} - \hat{\mathbf{\Phi}}_{k+1}$. *Then,* $\hat{\mathbf{P}}_{k+1|k+1}$ *is given by*

$$\hat{\mathbf{P}}_{k+1|k+1} = (\mathbf{I} - \mathbf{G}_{k+1}\hat{\mathbf{H}}'_{k+1})\hat{\mathbf{P}}_{k+1|k} + \mathbf{m}_{\mathbf{\Phi}}\mathbf{m}_{\mathbf{\Phi}}^{\mathrm{T}}, \forall k. \tag{32}$$

The result of Corollary 5.5 in (32) is important for the estimation of the control variable vector as shown in the next sub-section.

5.4. Estimation of Control Variable Vector

Using the corrected state vector $\hat{\mathbf{\Phi}}_{k+1}$ (Eq. (31)) and the covariance matrix of the state estimation error $\hat{\mathbf{P}}_{k+1|k+1}$ (Eq. (32)), the control variable vector $\hat{\mathbf{U}}_{k+1}$ ($\hat{\mathbf{U}}_{k+1} \equiv \begin{bmatrix} \hat{\mu}_{k+1} \\ \hat{\nu}_{k+1} \end{bmatrix}, \forall k$) can be estimated. The principles of stochastic optimal control theory and existing algorithms (Santina *et al*., 1994; Sheu, 2002) are applied to estimate $\hat{\mathbf{U}}_{k+1}$. Consistent with the principles of stochastic optimal control, the corrected state vector $\hat{\mathbf{\Phi}}_{k+1}$ is fed back through the optimal control gain matrix $\mathbf{\Theta}_{k+1}$ to determine the control variable vector $\hat{\mathbf{U}}_{k+1}$:

$$\hat{\mathbf{U}}_{k+1} = -\mathbf{\Theta}_{k+1}\hat{\mathbf{\Phi}}_{k+1} + \boldsymbol{\eta}_{k+1}, \forall k . \tag{33}$$

In Eq. (33), $\mathbf{\Theta}_{k+1}$ and $\boldsymbol{\eta}_{k+1}$ are given by

$$\mathbf{\Theta}_{k+1} = \left[\mathbf{B}_{k+1}^{\mathrm{T}}\mathbf{\Gamma}_{k+2}\mathbf{B}_{k+1} + \mathbf{\Psi}_{k+1}^{\mathrm{U}}\right]^{-1}\mathbf{B}_{k+1}^{\mathrm{T}}\mathbf{\Gamma}_{k+2}\hat{\mathbf{F}}'_{k+1}, \forall k , \tag{34}$$

$$\boldsymbol{\eta}_{k+1} = \left[\mathbf{B}_{k+1}^{\mathrm{T}}\mathbf{\Gamma}_{k+2}\mathbf{B}_{k+1} + \mathbf{\Psi}_{k+1}^{\mathrm{U}}\right]^{-1}\left[\mathbf{B}_{k+1}\mathbf{\Psi}_{k+1}^{\Phi}\mathbf{\Phi}_{k+1}^{*} + \mathbf{\Psi}_{k+1}^{\mathrm{U}}\mathbf{U}_{k+1}^{*}\right], \forall k , \tag{35}$$

where $\mathbf{B}_{k+1} = \left.\dfrac{\partial \mathbf{F}_{k+1}}{\partial \mathbf{U}_{k+1}}\right|_{\mathbf{U}_{k+1}=\hat{\mathbf{U}}_{k|k}}$ ($\forall k$), and matrix $\mathbf{\Gamma}_{k+2}$ should satisfy the Riccati equation as follows:

$$\mathbf{\Gamma}_{k+1} = \mathbf{\Psi}_{k+1}^{\Phi} + \mathbf{F}_{k+1}'^{\mathrm{T}}\mathbf{\Gamma}_{k+2}\mathbf{F}'_{k+1} - \mathbf{F}_{k+1}'^{\mathrm{T}}\mathbf{\Gamma}_{k+2}\mathbf{B}_{k+1}\mathbf{\Theta}_{k+1}, \forall k . \tag{36}$$

All of the system states that are characterized by the corrected state vector ($\hat{\mathbf{\Phi}}_{k+1}$) and the control variable vector ($\hat{\mathbf{U}}_{k+1}$) in time interval $k+1$ can be estimated using the aforementioned approach and the data that are collected through time interval $k+1$.

Utilizing the estimates of $\hat{\mathbf{\Phi}}_{k+1}$ and $\hat{\mathbf{U}}_{k+1}$, the state-dependent variables, including $\hat{X}_{k+1}$ and $\hat{Y}_{k+1}$ (by Theorem 4.1), together with Q_{k+1} (by Eq. (1)), can be updated and used as indices of the instantaneous performance of the system in terms of the efficiencies of the coordinated robots and the picker. Moreover, a picker's fatigue degree ($\hat{\rho}_{k+1}$) accumulated to time interval $k+1$ can be estimated (by Corollary 4.1 and Eq. (14)) in real time to determine whether it satisfies the boundary constraint (Eq. (4)) that protects the safety of the workers.

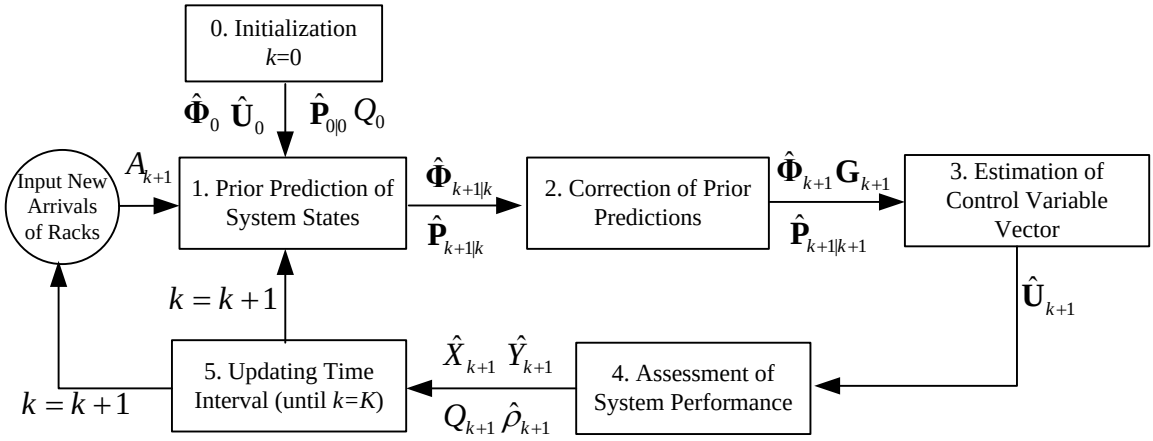

Fig. 2. Algorithmic procedures for data-driven real-time state estimation-control.

The proposed data-driven real-time state estimation-control approach can be coded in any appropriate computer programming language. This can not only facilitate the recursive calculation and optimal control of system states but also monitor system performance in real time. Figure 2 summarizes the primary algorithmic computational procedures based on the proposed approach.

6. REAL-PRACTICE BASED ANALYSIS

To demonstrate the validity and applicability of the proposed real-time data driven state estimation and control approach for robot-picker coordinated order fulfillment, data were collected from a dominant e-commerce company in China that uses robots for parts-to-picker order fulfillment. The data were obtained from a warehouse of that company, which is a 2,500m^2 robot-carried mobile-rack warehouse that stores small cosmetic items, in which 11 human pickers work with mobile robots to pick out customer orders. The raw data provide details about the pickers' picking and packaging tasks at the study site over six days in March, 2019. Data concerning the number of racks (A_k) that carry newly arriving SKUs to the storage area and the number of racks (Y_k) that are processed by each picker in the picking-packaging area in each time interval are used.

A total of 21 data sets which contain a total of 756 data points are generated from the collected raw data to facilitate real-time state estimation and control in this empirical study. Each data set contains 18 pairs of data points A_k and Y_k, measured every 10 minutes in a 3-hour task period. The data points A_k are inputs to, and Y_k are the measurements for the proposed approach. The generated 21 data sets are classified into three groups, associated with peak-hour, normal, and off-peak operational scenarios, respectively, to demonstrate the applicability of the proposed approach to diverse operational scenarios in order fulfillment centers. Specifically, seven, eight, and six data sets are obtained for *Scenarios* I (peak-hour), II (normal), and III (off-peak), respectively. Using the 21 data sets, the robot-picker coordinated order fulfillment performance and accumulated fatigue of the pickers in peak-hour, normal, and off-peak operational scenarios (*Scenarios* I, II, and III) are

comparatively analyzed.

Given the aforementioned 21 data sets (756 data points), the real-practice based empirical analysis is carried out through two phases to demonstrate the relative performance of the proposed robot-picker coordination mechanism for parts-to-picker order fulfillment.

The first phase of the empirical analysis aims to compare the results generated using the proposed approach with the measurements gained from the 21 data sets in the aspects of picker efficiency (the average of Y_k values) and accumulated fatigue (the average of ρ_K values). The comparative results are presented in Fig. 3, which help assess the relative performance of the proposed approach against the current parts-to-picker order fulfillment operations of the focal firm in the aspects of picker efficiency and fatigue alleviation, respectively.

Systems performance (Y_k and ρ_k)

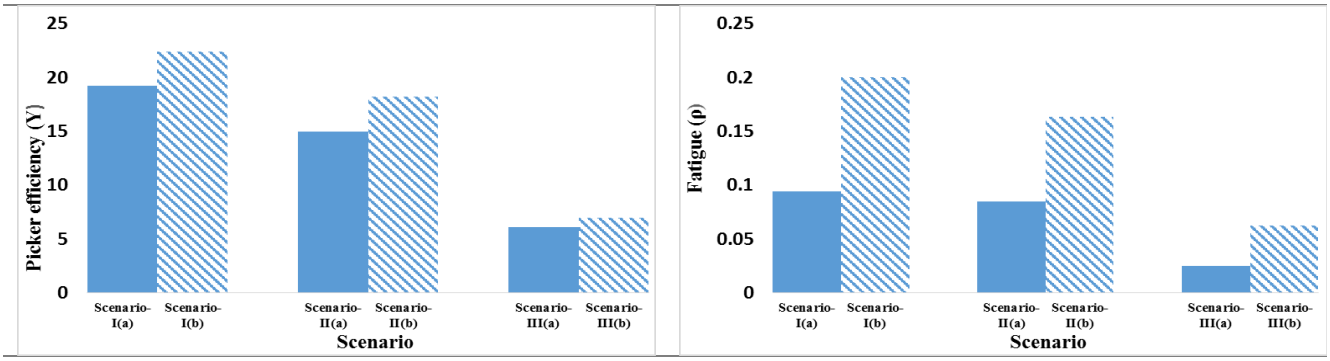

RP	-14.09%	-17.95%	-12.33%	-53.16%	-47.99%	-60.08%
ARP		-14.79%			-53.74%	

Scenarios: I, II, and III represent "peak", "normal", and "off-peak" scenarios; Indexes: a and b represent the scenarios "with" and "without" considering robot-picker coordination; RP: Relative performance; ARP: Average of relative performance

Fig. 3. Empirical results of phase I (robot-picker coordination relative to real operations).

Overall, the empirical results yielded in the first phase provide the following findings as summarized in Observation 6.1.

Observation 6.1. ***The proposed robot-picker coordination system permits alleviating a picker's fatigue in order fulfillment without much influence on picking efficiency, compared with the current performance of the focal firm in the study case*** — As can be seen in Fig. 3, a picker's accumulated fatigue can be reduced by 53.74% if the proposed robot-picker coordination system is applied in the focal firm of the study case. Such a fatigue alleviation, however, is carried out at the expense of lowering picker efficiency by 14.79%. Nevertheless, the above observation is encouraging for the applicability of the proposed method in practical cases of parts-to-picker order fulfillment systems as it implies that a more harmonious and enjoyable robot-human co-working environments can be created to facilitate the development of intelligent and human-friendly robot-human coordinated order fulfillment systems.

In the second phase of the empirical analysis, this work aims to demonstrate the relative performance of robot-picker coordination in contrast with the case without considering the robot-picker coordination for gaining more managerial implications. Therein, empirical results that are obtained with and without

consideration of the robot-picker coordination mechanism are compared. Without robot-picker coordination, both control variables μ_k and ν_k are set to 1 ($\mu_k = \nu_k = 1$) to mimic the current parts-to-picker order fulfillment operations of the focal firm of the case studied.

Figure 4 plots the empirical results concerning practice-based empirical analysis, including the average values of scenario-based state variables, control variables, system performance, and associated relative performance, as determined by comparing the outputs with and without robot-picker coordination. The findings and managerial implications of Fig. 4 are discussed below.

Observation 6.2. ***The proposed robot-picker coordination system outperforms the system without coordination in not only efficiency but also the fatigue of human pickers*** — As seen in Fig. 4, the relative performance (RP) values that are associated with γ_k in all three scenarios (peak-hour, normal, and off-peak scenarios) are positive, indicating that the pickers' working performance with robot-picker coordination is more efficient than without coordination. This higher efficiency is attributed to shorter queues racks (Q_k), owing to adjustments of the number of mobile racks that arrive at the picking and packaging area in each time interval based on estimates of the control variable μ_k in real time using the proposed approach. Additionally, the values of accumulated fatigue (ρ_k) that are found in all three scenarios with robot-picker coordination are lower than the scenarios without coordination. This observation is highly encouraging as it implies that customer orders can be efficiently fulfilled without the need for pickers to expend more energy and make more efforts while operating under the proposed robot-picker coordination, relative to the situation without it.

Observation 6.3. ***Robot-picker coordination improves system performance more in the "normal" scenario (Scenario II) than in the "peak-hour" and "off-peak" scenarios (Scenarios I and III)*** — This inference is drawn by comparing the RP values, particularly those associated with Q_k and ρ_k in the three scenarios. The "minus" signs of the RP values that are associated with Q_k and ρ_k imply that the proposed robot-picker coordination system alleviates pickers' accumulated fatigue ($\rho_k \downarrow$) by reducing the number of racks that queue ($Q_k \downarrow$) in the picking-packaging area. Such an effect of robot-picker coordination on either Q_k or ρ_k is highly significant under normal conditions (Scenario II) and is reasonable as the length of queues of racks (Q_k) is one of the key factors that is related to the stress and workloads of pickers, as captured by Eq. (3) in the proposed model.

1. State variables (γ_k and δ_k)

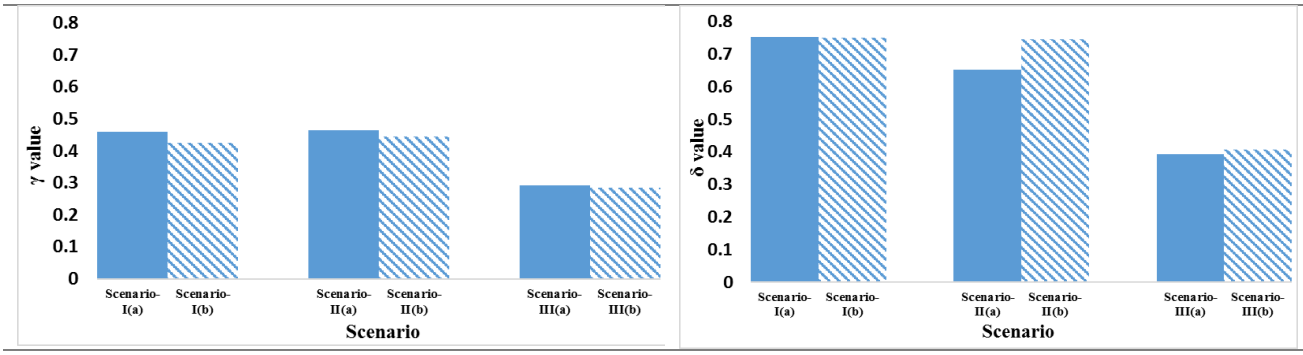

RP	7.84%	4.31%	1.24%	-0.31%	-10.28%	-1.98%

2. Control variables (μ_k and ν_k)

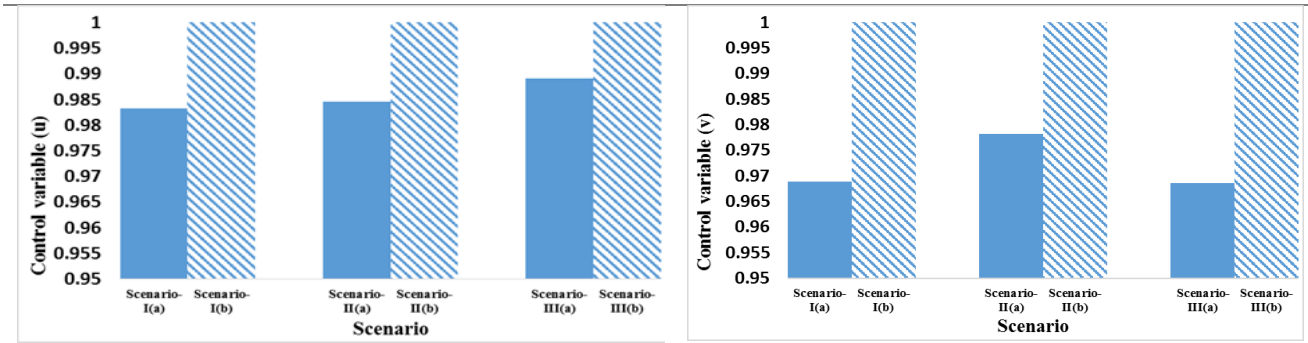

RP	-1.68%	-1.54%	-1.09%	-3.11%	-2.18%	-3.13%

3. Systems performance (Q_k , ρ_k , X_k , and Y_k)

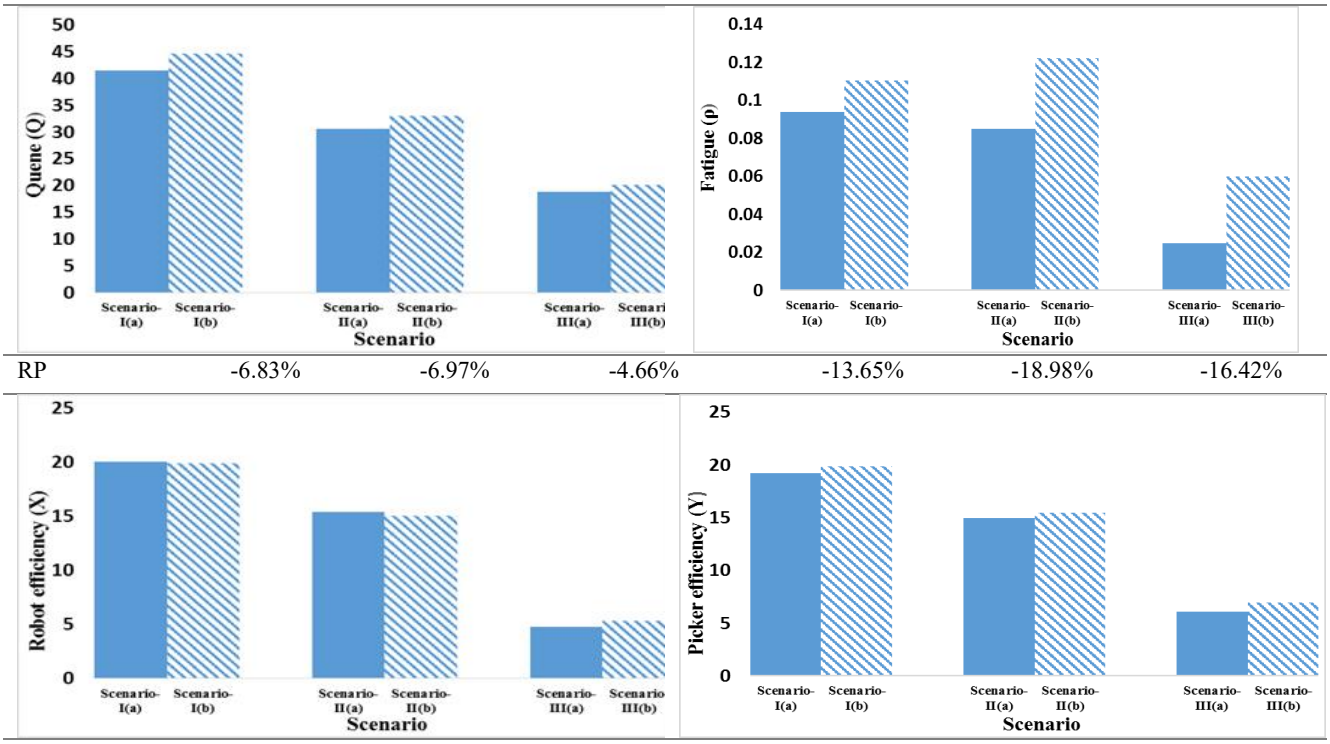

RP	-6.83%	-6.97%	-4.66%	-13.65%	-18.98%	-16.42%
RP	0.77%	1.44%	-7.31%	-3.16%	-3.54%	-7.73%

Scenarios: I, II, and III represent "peak", "normal", and "off-peak" scenarios; Indexes: a and b represent the scenarios "with" and "without" considering robot-picker coordination; RP: Relative performance

Fig. 4. Empirical results of phase II (robot-picker coordination performance).

Observation 6.4 (Human-friendly robot behavior for coordination with human pickers in different operational scenarios). ***Under the proposed robot-picker coordination, robots can exhibit different***

coordination behaviors in response to the instantaneous performance of coordinated pickers in different scenarios, as follows.

(a) ***Under peak-hour conditions (Scenario I)*** *— Robots tend to handle racks with high efficiency (by increasing* X_k *value) in the storage area, and this efficiency almost matches the coordinated picker's efficiency in processing racks (* $X_k \approx Y_k$ *). Moreover, robots tend to stabilize the volume of racks that are delivered to the coordinated pickers (by stabilizing* μ_k *value); meanwhile, the rack volume that is returned to the storage area is adjusted (by reducing* ν_k *value), based on the coordinated pickers' instantaneous efficiency (by estimating* Y_k *value). Consequently, the accumulated number of queuing racks in the picking-packaging area can be well controlled (by reducing the* Q_k *value) to mitigate the accumulated stress and fatigue of coordinated human pickers during peak hours.*

(b) ***Under normal conditions (Scenario II)*** *— Robots adjust their efficiency of handling racks in the storage area to keep the number of racks that are moved to the picking-packaging area almost equal to the number of racks that are processed by the coordinated pickers (* $X_k \approx Y_k$ *) per unit time such that the accumulated number of racks that queue in the picking-packaging area remains stable. (*Q_k *remains approximately double the value of* Y_k *in this case). Meanwhile, the volumes of mobile racks (carried by robots) that move between the storage and picking-packaging areas are controlled to be almost equal to each other (* $\mu_k \approx \nu_k$ *).*

(c) ***Under off-peak conditions (Scenario III)*** *— Robots handle racks in the storage area more slowly (by reducing* X_k *value) to keep their efficiency a little lower than the coordinated pickers' efficiency in processing racks (* $X_k \leq Y_k$ *). Meanwhile, the volumes of racks that are moved between the storage area and the picking-packaging area are adjusted in response to the coordinated picker's processing of racks. Specifically, robots tend to move racks forward fast (by increasing* μ_k *value), and to return racks from the picking-packaging area more slowly (by reducing* ν_k *value) during off-peak hours.*

Three empirical examples, based on three selected datasets, are further used to present graphically the aforementioned characteristics of robot-picker coordination behavior that is typically exhibited during "peak", "normal" and "off-peak" hours, as shown in Figs. 5 to 7. Briefly, the coordinated robots adjust their efficiency (X_k) in handling racks in the storage area, and controlling the volumes of racks (by μ_k and ν_k) that move between the storage area and the picking-packaging area in response to the coordinated pickers' efficiency in processing racks (by Y_k) and accumulated fatigue (ρ_k). Under such a proposed robot-picker coordination, the lengths of the queues of racks in the picking-packaging area can also be controlled.

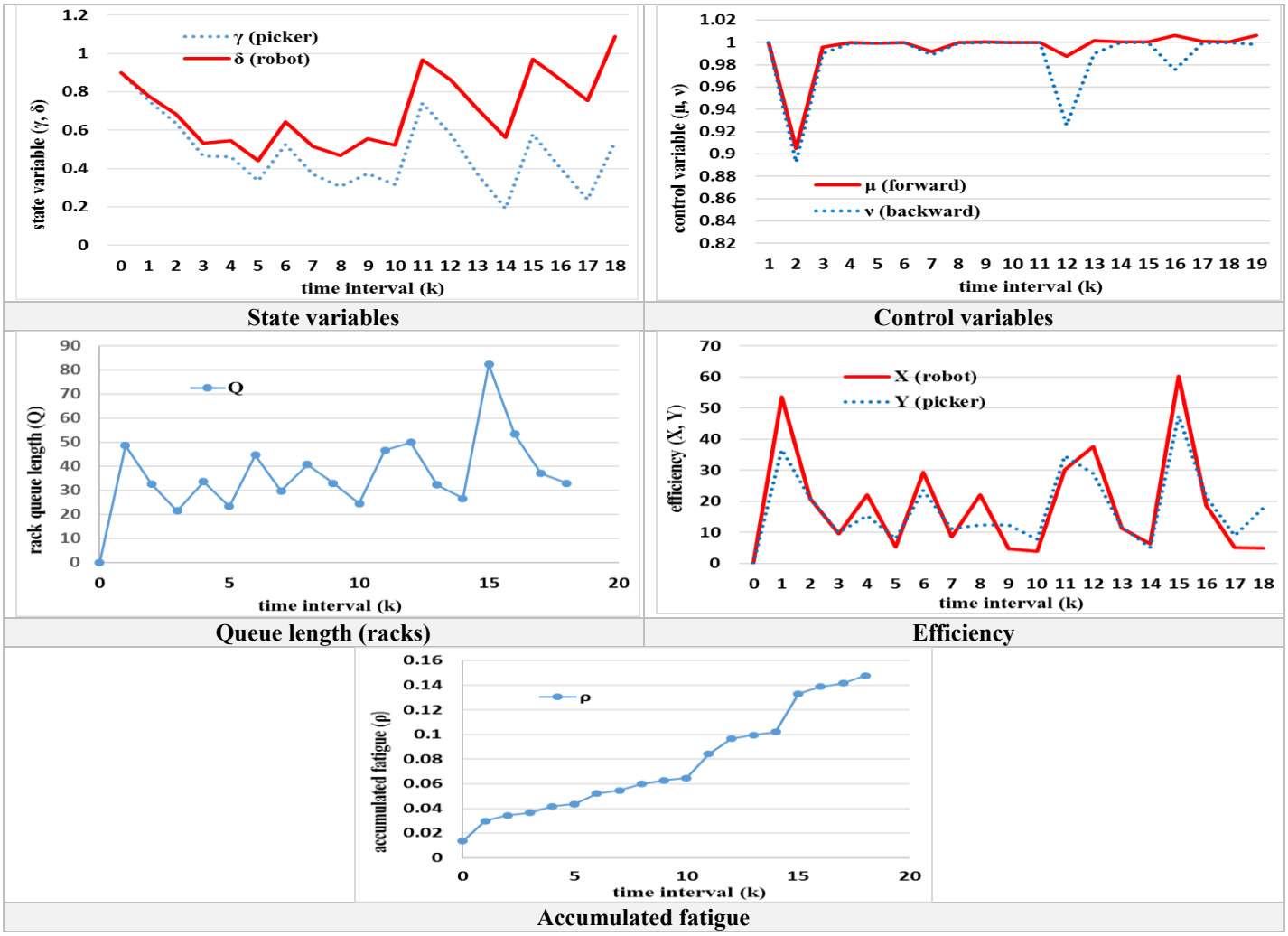

Fig. 5. Empirical example (1) — system output during peak hours (Scenario I)

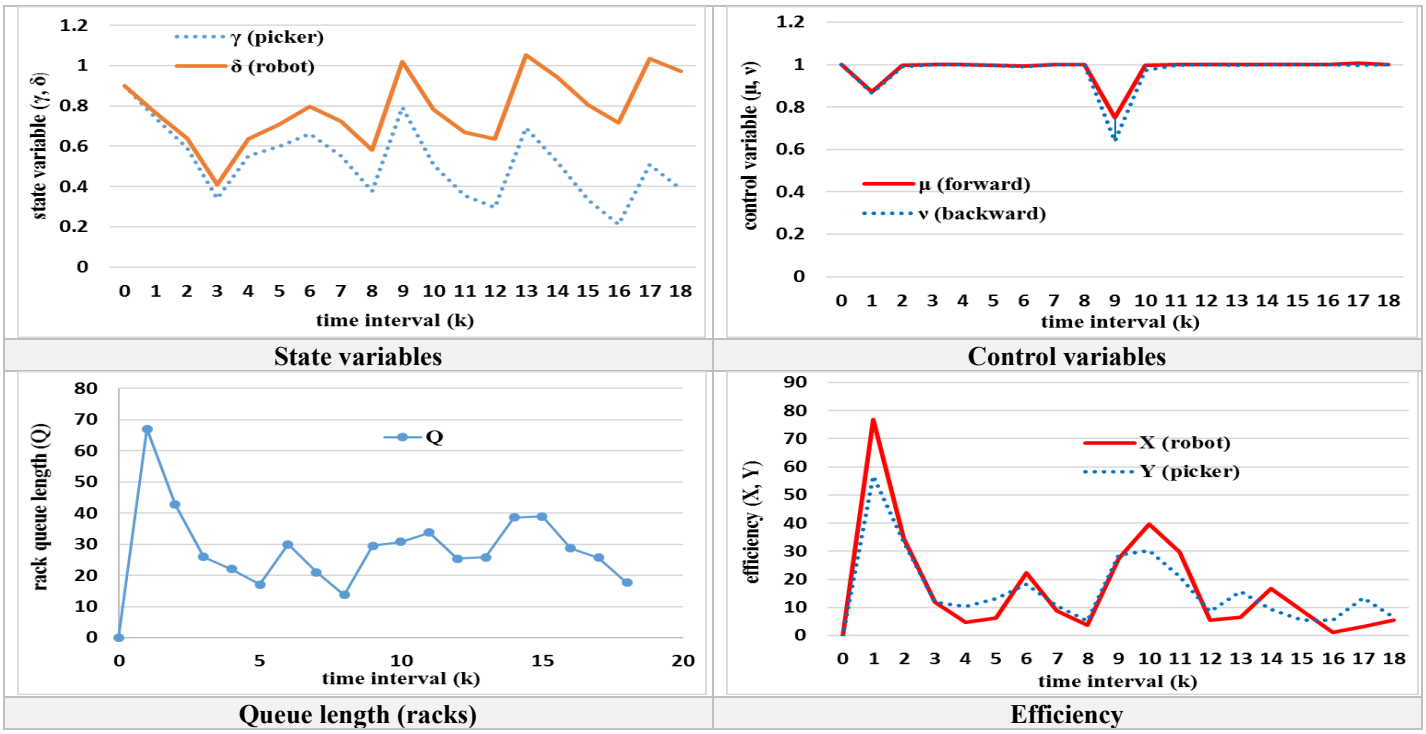

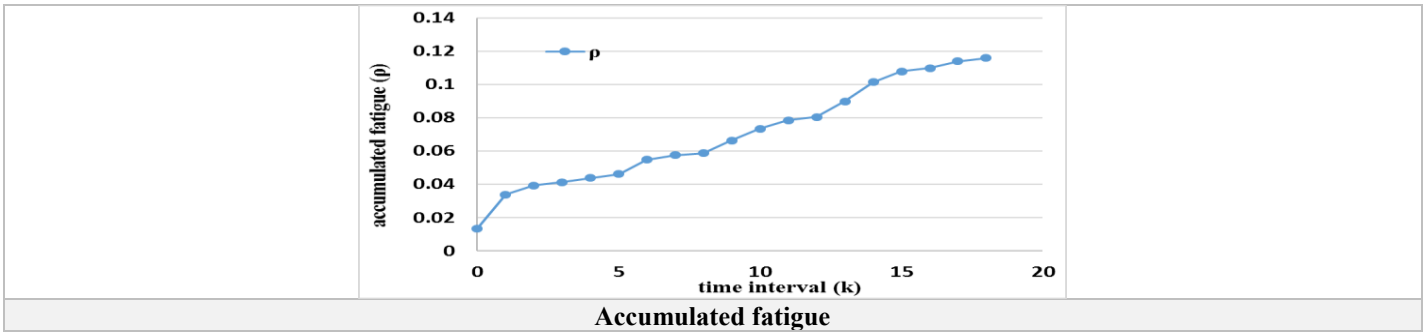

Fig. 6. Empirical example (2) — system output during normal hours (Scenario II).

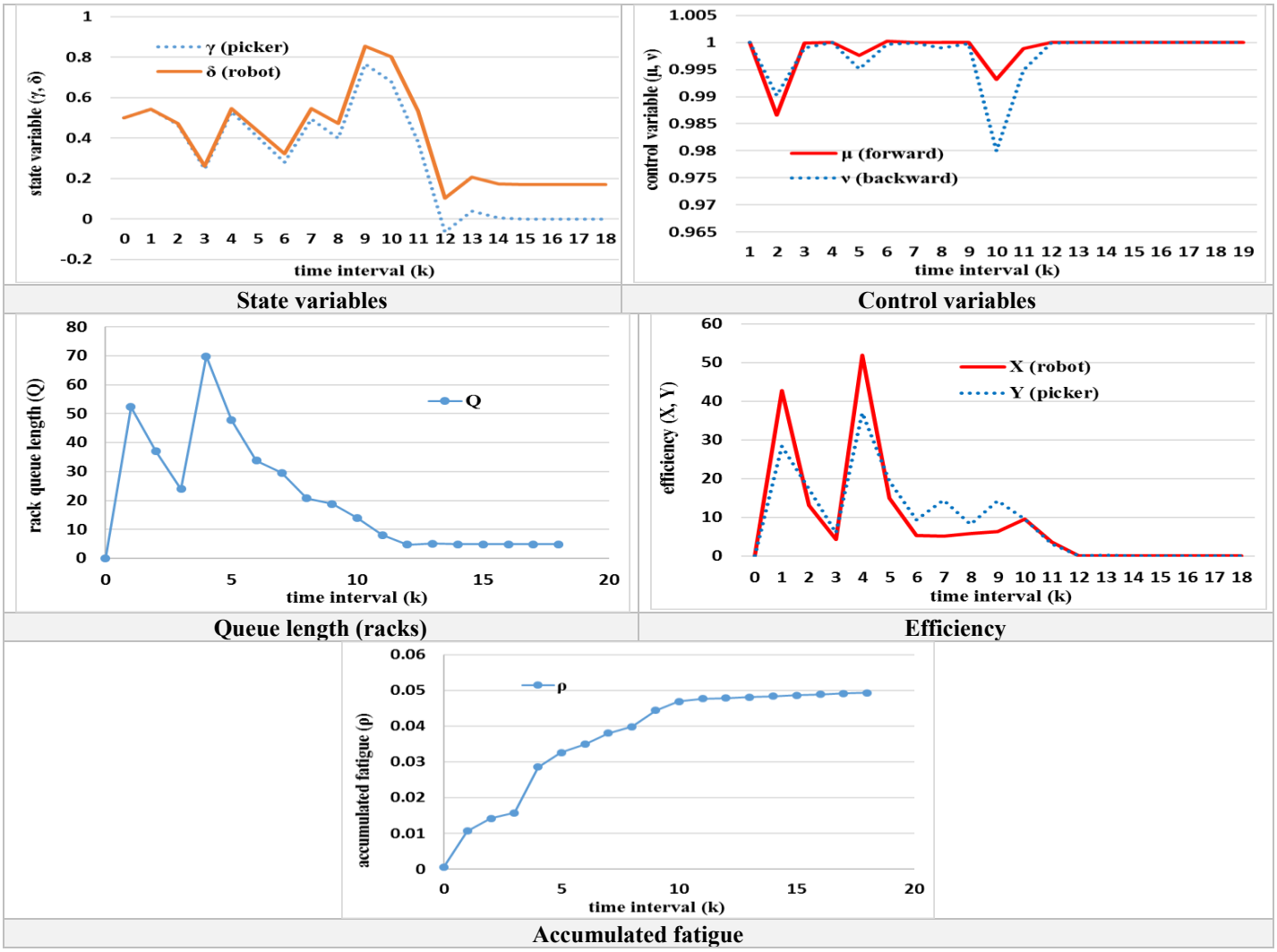

Fig. 7. Empirical example (3) — system output during off-peak hours (Scenario III).

The results concerning empirical example 1 (Fig. 5) reveal a large difference between accumulated fatigue (ρ_k) in a 3-hour peak period in Scenario I and those shown in the other two scenarios. Thus, Scenario I is used to conduct sensitivity analysis on two key parameters (β_1 , and β_2) which determine the effects of picker efficiency (Y_k) and rack queue length (Q_k), respectively, on the fatigue growth rate (λ_k), as captured by Eq. (3). The parameter settings ($\beta_1 = 0.00005$ and $\beta_2 = 0.00005$) and dataset that are used in empirical example 1 provide the baseline in the sensitivity analysis. Figure 8 plots the empirical results of the sensitivity analysis of

the relationships among ρ_k, β_1, and β_2, where the value of ρ is the average of the ρ_k values that are estimated during the 3-hour peak period. Figure 8 has managerial implications concerning the psychological and physical effects of workload on human pickers, which are determined by the perceived rack queue lengths and the picking efficiency of pickers in coordination with robots during peak hours.

Observation 6.5. ***A picker's accumulated fatigue (ρ) increases significantly with either the picker's efficiency (Y_k) or perceived rack queue length (Q_k) during peak hours; the increase in ρ with Q_k exceeds that with Y_k.***

During peak hours, a human picker is likely to be more sensitive to the perceived length of the queue of unprocessed mobile racks than to the number of racks processed. Therefore, perceiving any anomalous increase in the length of the queue of mobile racks would easily have a negative effect on the picker's psychological and behavioral responses (such as stress, anxiety, and panic).

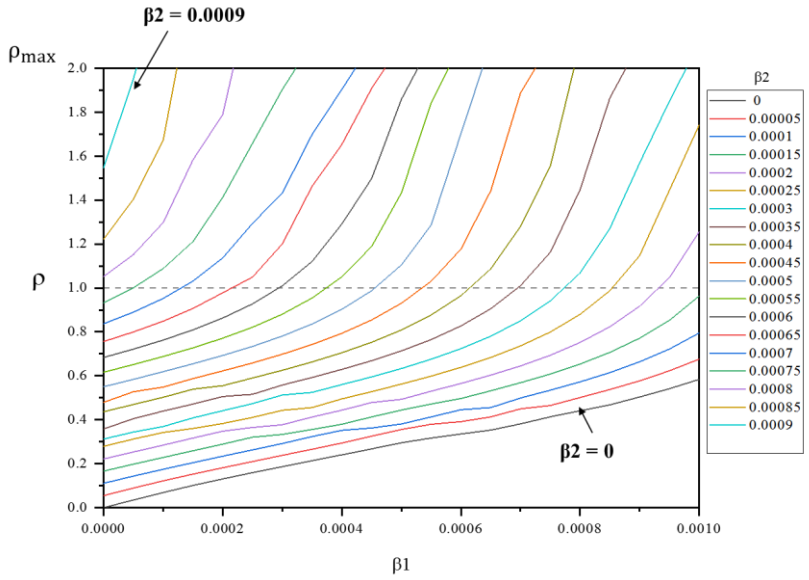

Fig. 8. Sensitivity analysis of ρ (with respect to β_1 and β_2) in peak-hour scenario.

7. CONCLUSIONS, MANAGERIAL IMPLICATIONS AND RECOMMENDATIONS

7.1 Conclusions

Motivated by the introduction of robots and advanced technologies into intelligent logistics operations and the impact thereof on worker safety and well-being, this work has presented a real-time data-driven stochastic optimal control-based approach to addressing the issue of robot-picker coordinated order fulfillment. Specifically, the proposed approach combines a discrete-time nonlinear stochastic-dynamic model with a fatigue accumulation function (Section 4) in a real-time system state estimation and control method (Section 5) to find the optimal solutions for the coordination between human pickers and robots. Theoretically and in practice, the coordinated robots can react and adapt to picker efficiency in real time, such that the coordinated robots and

pickers can jointly fulfill orders in collaboration and in a human-friendly manner. Sections 4 and 5 have presented the methodological characteristics and novelty of the proposed approach, which may help address the first research question raised in Section 1. To answer the second question (Section 1), an empirical analysis has been performed using actual data that were collected from a dominant e-commerce company in China that uses robots for "parts-to-picker" order fulfillment. An empirical study has been conducted to generate various insights (called "observations") which help answer the second question, concerning how the proposed human-friendly, robot-human coordination system improves the performance of a parts-to-picker order fulfillment center in terms of both safety and human well-being.

7.2. Managerial Implications

The analytical results that were obtained using the proposed model (Sections 4 and 5) and the empirical results of the empirical analysis of actual data (Section 6) provide the following managerial implications.

Implication 1. ***Under the proposed robot-picker coordinated order fulfillment mechanism, the robot and picker efficiencies (X_k and Y_k) have the following characteristics.***

(a) ***The robot and picker efficiencies (X_k and Y_k) can be effectively controlled and coordinated if real-time data concerning newly arriving racks (A_k) that are loaded with SKUs are obtained.***

(b) ***Robot efficiency (X_k) depends strongly on A_k whereas picker efficiency (Y_k) depends strongly on the length of the queue of unprocessed racks (Q_k).***

The above managerial insights are based on Theorem 4.1, Observations 6.2 and 6.5. The effect of the perceived length of the queue (Q_k) of unprocessed racks on systems performance is emphasized and has implications for operations managers (*e.g.*, in warehousing), enabling them better to manage the number of racks in queues by appropriately controlling the speeds with which robots deliver racks to the picking-packaging area.

Implication 2. ***Under the proposed robot-picker coordinated order fulfillment mechanism, the picker-to-robot relative performance in the aspect of either efficiency (Y_k/X_k) or effectiveness (γ_k/δ_k) in peak hours is less than that in either normal or off-peak hours. The picker-to-robot relative performance is greatest in the "off-peak" scenario.*** This implication is drawn from a comparison of empirical results (Fig. 4) for Y_k/X_k and γ_k/δ_k among the three scenarios. It may help operations managers to determine appropriate criteria and standards for evaluating the efficiency and effectiveness of pickers in different scenarios.

Implication 3. ***Robot efficiency is not the most important metric. Rather, human efficiency dominates the efficiency of a parts-to-picker order fulfillment system, particularly during peak hours. Accordingly, controlling the number of queued racks by slowing down their delivery by robots to the picking-packaging area is more efficient than slowing down the rack-processing of a picker to alleviate that picker's fatigue, particularly during a peak-hour period***. This implication is drawn from the empirical results (Fig. 8), and is consistent with Observation 6.5 and Insight 1(b). It suggests the importance of accounting for human well-being and safety in the design and implementation of a human-friendly intelligent robot-human coordinated order

fulfillment system. In such a system, humans are the key element and robots should be sufficiently intelligent and accommodating to assist humans in the joint intelligent logistics task of order fulfillment.

7.3. Recommendations for Future Research

Despite the novelty of the proposed methodology and its advantages in realizing a human-friendly intelligent robot-human coordinated order fulfillment system, this research has several limitations. First, the proposed model has not incorporated factors related to worker psychology (*e.g*., perceived job worth, job attitude, and emotional involvement) and behavior (*e.g*., body posture) toward coordination and cooperation with robots, and these factors should be further explored and empirically verified in the future (MacDonald, 2013; Tan and Netessine, 2014; Tan *et al*., 2021). For example, body posture is regarded as a kind of physical demands which may contribute to psychosocial hazards (*i.e*., negative effects on employees such as stress and health problems), as claimed in MacDonald (2013). Thus, body posture can be another issue to improve employees' stress and health problems in human-robot collaborative work settings. Other related tasks that are undertaken in inbound logistics (such as storage assignment) and outbound logistics (such as resource/fleet management, vehicular loading, dispatching, and routing) have not yet been considered. They may be worthy of further investigation. Extending the proposed model for the cases of multiple working periods intervened by scheduled breaks is analytically challenging yet meaningful for future research. Last but not least, considering how robotics can be used to help cope with capacity bottlenecks and supply chain disruptions due to manpower shortage under/after the COVID-19 pandemic (Gupta *et al*. 2022) will also be interesting to study in the future.

References

All cited URLs were last accessed on 1st February 2022.

Al Elew, M, S. Oh. 2020. What are injury rates like at Amazon warehouses. Reveal News, September 29, 2020. Available at https://revealnews.org/article/amazon-injury-rates/.

Anderson, Jr. E.G., D.J. Morrice, G. Lundeen. 2006. Stochastic optimal control for staffing and backlog policies in a two-stage customized service supply chain. *Production and Operations Management* 15(2), 262-278.

Azadeh, K., R. De Koster, D. Roy. 2019. Robotized and automated warehouse systems: Review and recent developments. *Transportation Science* 53(4), 917-945.

Banker, S. 2016. Robots in the warehouse: It's not just Amazon. Forbes, January 11, 2016. Available at https://www.forbes.com/sites/stevebanker/2016/01/11/robots-in-the-warehouse-its-not-just-amazon/#1bd3d6e540b8.

Barrett, M., E. Oborn, W.J. Orlikowski, J. Yates. 2012. Reconfiguring boundary relations: Robotic innovations in pharmacy work. *Organization Science* 23(5), 1448-1466.

Batt, R.J., S. Gallino. 2019. Finding a needle in a haystack: The effects of searching and learning on pick-worker performance. *Management Science* 65(6), 2624-2645.

Beane, M., W.J. Orlikowski. 2015. What difference does a robot make? The material enactment of distributed coordination. *Organization Science* 26(6), 1553-1573.

Boldrer, M., A. Antonucci, P. Bevilacqua, L. Palopoli, D. Fontanelli. 2022. Multi-agent navigation in human-

shared environments: A safe and socially-aware approach. *Robotics and Autonomous Systems* 149, 103979.

Boysen, N., D. Briskorn, S. Emde. 2017. Parts-to-picker based order processing in a rack-moving mobile robots environment. *European Journal of Operational Research* 262, 550-562.

Bozer, Y.A., F.J. Aldarondo. 2018. A simulation-based comparison of two goods-to-person order picking systems in an online retail setting. *International Journal of Production Research* 56(11), 3838-3858.

Bureau of Labor Statistics. 2014. Nonfatal Occupational Injuries and Illnesses Requiring Days Away from Work, 2013. USDL-14-2246. Washington, DC: United States Department of Labor.

Chen, C.-M., Y. Gong, R.B.M. de Koster, J.A.E.E. van Nunen. 2010. A flexible evaluative framework for order picking systems. *Production and Operations Management* 19(1), 70-82.

Chen, Y., C. Yang, Y. Gu , B. Hu. 2022. Influence of mobile robots on human safety perception and system productivity in wholesale and retail trade environments: A pilot study. *IEEE Transactions on Human-Machine Systems* 52(4), 624-635.

Choi, T.M., Kumar, S., Yue, X., Chan, H.L. 2022. Disruptive technologies and operations management in the industry 4.0 era and beyond. *Production and Operations Management* 31(1), 9-31.

Chung, S.H. 2021. Applications of smart technologies in logistics and transport: A review. *Transportation Research Part E* 153, 102455.

Cooper, R., M. Foster.1971. Sociotechnical systems. *American Psychologist* 26(5), 467-474

Del Rey, J. 2019. How robots are transforming Amazon warehouse jobs — for better and worse. Vox, December 11, 2019. Available at https://www.vox.com/recode/2019/12/11/20982652/robots-amazon-warehouse-jobs-automation.

De Koster, R., T. Le-Duc, K.J. Roodbergen. 2007. Design and control of warehouse order picking: A literature review. *European Journal of Operational Research* 182(2), 481-501.

De Vries, J., R. de Koster, D. Stam. 2016. Aligning order picking methods, incentive systems, and regulatory focus to increase performance. *Production and Operations Management*, 25(8), 1363-1376.

Demaitre, E. 2019. Geek+ raises another $150M for global expansion of autonomous mobile robots. The Robot Report, July 11, 2019. Available at https://www.therobotreport.com/geek-raises-funds-autonomous-mobile-robots/.

Do, H.T., M. Shunko, M.T. Lucas, D.C. Novak. 2018. Impact of behavioral factors on performance of multi-server queueing systems. *Production and Operations Management* 27(8), 1553-1573.

Doll, S. 2020. Amazon's automated warehouses have reportedly led to more worker injuries. Screen Rant, September 29, 2020. Available at https://screenrant.com/amazon-automated-warehouses-worker-injuries-increase-report/.

Drury, J. 1988 Toward more efficient order picking. Technical Report 1, Institute of Materials Management, Cranfield, UK.

Enright, J., P. Wurman. 2011. Optimization and coordinated autonomy in mobile fulfillment systems. In *Workshops at the twenty-fifth AAAI conference on artificial intelligence*. 2011.

Evans, W. 2020. How Amazon hid its safety crisis. Reveal News, September 29, 2020. Available at https://revealnews.org/article/how-amazon-hid-its-safety-crisis/.

Faraj, S., Y. Xiao. 2006. Coordination in fast-response organizations. *Management Science* 52(8), 1155-1169.

Frazelle, E. A. 2002. *World-class Warehousing and Material Handling*, McGraw-Hill, New York.

Garland, 2022. Amazon unveils first fully autonomous mobile robot. Supplychain Dive, June 28, 2022. Available at https://www.supplychaindive.com/news/amazon-unveils-first-fully-autonomous-mobile-robot-proteus-warehouse/626164/.

Gharehgozli, A., N. Zaerpour. 2020. Robot scheduling for pod retrieval in a robotic mobile fulfillment system. *Transportation Research Part E* 142, 102087.

Glock, C.H., E.H. Grosse, H. Abedinnia, S. Emde. 2019a. An integrated model to improve ergonomic and economic performance in order picking by rotating pallets. *European Journal of Operational Research* 273(2), 516-534.

Glock, C.H., E.H. Grosse, T. Kim, W.P. Neumann, A. Sobhani. 2019b. An integrated cost and worker fatigue evaluation model of a packaging process. *International Journal of Production Economics* 207, 107-124.

Grosse, E.H., C.H. Glock. 2015. The effect of worker learning on manual order picking processes. *International Journal of Production Economics* 170, 882-890.

Grosse, E.H., C.H. Glock, M.Y. Jaber, W.P. Neumann. 2015. Incorporating human factors in order picking planning models: framework and research opportunities. *International Journal of Production Research* 53 (3), 695-717.

Grosse, E.H., C.H. Glock, W.P. Neumann. 2017. Human factors in order picking: a content analysis of the literature. *International Journal of Production Research* 55(5), 1260-1276.

Gupta, S., M.K. Starr, R. Zanjirani Farahani, N. Asgari. 2022. Pandemics/epidemics: Challenges and opportunities for operations management research. *Manufacturing & Service Operations Management* 24(1), 1-23.

Hinds, P.J., T.L. Roberts, H. Jones. 2004. Whose job is it anyway? A study of human-robot interaction in a collaborative task. *Human-Computer Interaction* 19(1), 151-181.

Jaber, M.Y., Z.S. Givi, W.P. Neumann. 2013. Incorporating human fatigue and recovery into the learning–forgetting process. *Applied Mathematical Modelling* 37, 7287-7299.

Karuppan, C.M., M.J. Schniederjans. 1995. Sources of stress in an automated plant. *Production and Operations Management* 4(2), 108-126.

Kc, D.S., C. Terwiesch. 2009. Impact of workload on service time and patient safety: An econometric analysis of hospital operations. *Management Science* 55(9), 1486-1498.

Lamballais, T., D. Roy, M.B.M. de Koster. 2017. Estimating performance in a Robotic Mobile Fulfillment System. *European Journal of Operational Research* 256, 976-990.

Larco, J.A., R. de Koster, K.J. Roodbergen, J. Dul. 2017. Managing warehouse efficiency and worker discomfort through enhanced storage assignment decisions. *International Journal of Production Research* 55(21), 6407-6422.

Lavender, S.A., W.S. Marras, S.A. Ferguson, R.E. Splittstoesser, G. Yang. 2012. Developing physical exposure-based back injury risk models applicable to manual handling jobs in distribution centers. *Journal of Occupational and Environmental Hygiene* 9(7), 450–459.

Li, X., G. Hua, A. Huang, J.-B. Sheu, T.C.E. Cheng, F. Huang. 2020. Storage assignment policy with awareness of energy consumption in the Kiva mobile fulfilment system. *Transportation Research Part E* 144, 102158.

Loffler, M., N. Boysen, M. Schneider. 2022. Picker routing in AGV-assisted order picking systems. *INFORMS Journal on Computing* 34(1), 440-462.

Loske, D. 2022. Empirical evidence on human learning and work characteristics in the transition to automated order picking. Journal of Business Logistics 43(3), 302-342.

Luo, S., T.M. Choi. 2022. E-commerce supply chains with considerations of cyber-security: Should governments play a role? *Production and Operations Management* 31(5), 2107-2126.

MacDonald, W. 2003. The impact of job demands and workload on stress and fatigue. *Australian Psychologist* 38(2), 102-117.

Mumford, E. 2006. The story of socio-technical design: reflections on its successes, failures and potential. *Information Systems Journal* 16(4), 317-342.

Olsen, T.L., B. Tomlin. 2020. Industry 4.0: Opportunities and challenges for operations management. *Manufacturing and Service Operations Management* 22(1), 113-122.

Perera, S., M. Dawande, G. Janakiraman, V. Mookerjee. 2020. Retail deliveries by drones: How will logistics networks change? *Production and Operations Management* 29(9), 2019-2034.

Rai, R., M.K. Tiwari, D. Ivanov, A. Dolgui. 2021. Machine learning in manufacturing and industry 4.0 applications. *International Journal of Production Research* 59 (16), 4773-4778.

Rosenthal, S.R. 1984. Progress toward the factory of the future. *Journal of Operations Management* 4(3), 203-229.

Santina, M.S., A.R. Stubberud, G.H. Hostetter. 1994. *Stochastic Systems and Recursive Estimation*, (Edited by M. S. Santina *et al.*), Digital Control System Design, pp. 580-679. Saunders College Publishing, Harcourt Brace College Publishers, San Diego.

Sheu, J.-B. 2002. A stochastic optimal control approach to real-time incident-responsive traffic signal control at isolated intersections. *Transportation Science* 36(4), 418-434.

Shi, Y., H. Yu, Y. Yu, X. Yue. 2021. Analytics for IoT-enabled human–robot hybrid sortation: an online optimization approach. *Production and Operations Management.* https://doi.org/10.1111/poms.13626.

Tam, D. 2014. Meet Amazon's busiest employee – the Kiva robot. CNET, November 30, 2014. Available at http://www.cnet.com/news/meet-amazons-busiest-employee-the-kiva-robot/.

Tan, P.M., J. Koopman, S.T. McClean, J.H. Zhang, C.H. Li, D. De Cremer, Y. Lu, C.T.S. Ng. 2022. When conscientious employees meet intelligent machines: An integrative approach inspired by complementarity theory and role theory. *Academy of Management Journal* 65(3), 1019-1054.

Tan, T.F., S. Netessine. 2014. When does the devil make work? an empirical study of the impact of workload on worker productivity. *Management Science* 60(6), 1574-1593.

Tobe, F. 2018. Warehousing, fulfillment and DC transformation trends. The Robot Report, May 6, 2018. Available at https://www.therobotreport.com/warehousing-fulfillment-and-dc-transformation-trends/.

Tompkins, J.A., J.A. White, Y.A. Bozer, J.M.A. Tanchoco. 2010. Facilities Planning. John Wiley & Sons, Hoboken, NJ.

Wang, Z., J.-B. Sheu, C.-P. Teo, G. Xue. 2022. Robot scheduling for mobile-rack warehouses: human-robot coordinated order picking systems. *Production and Operations Management* 31(1), 98-116.

Weidinger, F., N. Boysen, D. Briskornb. 2018. Storage assignment with rack-moving mobile robots in KIVA warehouses. *Transportation Science* 52(6), 1479-1495.

Yuan, R., S.C. Graves, T. Cezik. 2019. Velocity-based storage assignment in semi-automated storage systems. *Production and Operations Management* 28(2), 354-373.